


For Reference

NOT TO BE TAKEN FROM THIS ROOM

Ex libris
UNIVERSITATIS
ALBERTAENSIS





Digitized by the Internet Archive
in 2023 with funding from
University of Alberta Library

<https://archive.org/details/Guillaume1977>

THE UNIVERSITY OF ALBERTA

RELEASE FORM

Name of Author: A.R.A. Guillaume

Title of Thesis: Drift and Random Velocities in a Hot Plasma

Degree for which thesis was presented: Master of Science

Year this degree granted: Spring 1977

Permission is hereby granted to THE UNIVERSITY OF ALBERTA LIBRARY to reproduce single copies of this thesis and to lend or sell such copies for private, scholarly or scientific research purposes only.

The author reserves other publication rights, and neither the thesis nor extensive extracts from it may be printed or otherwise reproduced without the author's written permission.

THE UNIVERSITY OF ALBERTA

Drift and Random Velocities
In A Hot Plasma

By



A.R.A. Guillaume

A Thesis

Submitted to the Faculty of Graduate Studies and Research
In Partial Fulfilment of the Requirements for the Degree
of Master of Science

Department of Electrical Engineering

Edmonton, Alberta

Spring, 1977

THE UNIVERSITY OF ALBERTA
FACULTY OF GRADUATE STUDIES AND RESEARCH

The undersigned certify that they have read, and recommend to the Faculty of Graduate Studies and Research, for acceptance, a thesis entitled "Drift and Random Velocities In a Hot Plasma", submitted by August R.A. Guillaume in partial fulfilment of the requirements for the degree of Master of Science in Electrical Engineering.

Abstract

This thesis deals with instabilities found in the infinite, collisionless, homogeneous plasma with no external fields. The plasma has random motion and contains an arbitrary number of streams, each stream having its own mass, temperature and streaming velocity. The region of validity of Landau damping is found to include disturbances with phase velocities greater than two and one half times the thermal velocity in one-component plasmas. It is concluded that marginal inverse Landau damping cannot explain the two stream instability. Based on analysis of the dispersion relation and numerical solutions on the computer, instability is found to increase when the largest streaming velocity is increased or the largest Debye number is decreased in a multi-component plasma.

ACKNOWLEDGEMENTS

The author acknowledges with thanks the encouragement and guidance received from his supervisors, Dr. C.R. James and Dr. C.E. Capjack through the course of this research. Thanks are also due to the Department of Electrical Engineering for the financial support that made this work possible. Computational facilities were of great help. The author owes a debt of gratitude to his wife for her patience and to Barb Galliaford who struggled faithfully through the equations and symbols while typing this manuscript.

TABLE OF CONTENTS

CHAPTER 1	INTRODUCTION	PAGE
	1.1 Purpose and Scope	1
CHAPTER 2	DERIVATION OF THE DISPERSION RELATION	4
	2.1 Basic Equations	4
	2.2 The Velocity Distribution Function	7
	2.3 The Dispersion Relation	9
	2.4 Longitudinal Waves	12
	2.5 Transverse Waves	16
	2.6 Qualitative Discussion of the Dispersion Relations	19
	2.7 Effect of Parameters on Distribution Function	25
	2.8 Physical Interpretation Review	33
CHAPTER 3	QUANTITATIVE DISCUSSION	35
	3.1 General	35
	3.2 The "One-Component" Plasma	36
	3.3 Two Stream Instability	38
	3.4 Multi-Component Plasmas	67
CHAPTER 4	SUMMARY	76
	FOOTNOTES	78
	BIBLIOGRAPHY	79
	APPENDIX	80
	Plasma Dispersion Relation	80

LIST OF TABLES

		PAGE
3.3.1 - 3.3.15	Instability of a Multi-Component Plasma	46
3.3.16	Instability of a Two-Component Plasma	66
3.4.1 - 3.4.5	Four-Stream Plasmas	67
3.4.6 - 3.4.13	Three-Stream Plasmas	70
3.4.14	Comparisons	74

LIST OF FIGURES

	PAGE
Figure 1.1 $Z(z)$ for real z between -5 and $+5$	18
Figure 1.2 $Z'(z)$ for real z between -5 and $+5$	20
Figure 2 Upper Half z_σ plane	24
Figure 3 Values of z_L and z_S for various k_{D_i}/k_{D_j}	44
Figure 4 Marginal Stability	61
Figure 5 Marginal Stability	64
Figure 6 Marginal Stability	65

Chapter 1

INTRODUCTION

1.1 Purpose and Scope

Particle wave interactions in a hot plasma have been under intense investigation ever since Landau¹ theoretically predicted that spontaneous oscillations are damped even though there are no collisions. It is well known² that such microscopic collisionless damping is caused by particles absorbing energy from the disturbing wave when they are travelling slightly slower than its phase velocity. Conversely particles may give energy to the wave by travelling slightly faster than the phase velocity. This effect tends to cause the wave to grow. Normally both these effects are present and it is a matter of which one dominates that determines whether the wave damps or grows.

Such microscopic phenomena occur when there is a distribution in random motion. On the other hand macroscopic bunching occurs when drift motion is present. This instability is caused by density fluctuations in the plasma. (see section 2.8). This thesis will investigate plasmas where both random motion and drift motion are present. One of the objectives of the thesis will be to determine the conditions under which each interaction dominates. As well, a method for determining the stability of a multi-component plasma will be given.

The model to be considered is a hot multi-component plasma, each component with its own velocity distribution, density, temperature, mass, and streaming velocity. The plasma is infinite and homogeneous throughout, with no external electric or magnetic fields.

Only two types of free energy sources to feed the instability will be considered. The first, the macroscopic source, is derived from the drift kinetic energy associated with each of the beams of particles in the plasma. The beams are streaming with velocities relative to each other. This is the macroscopic source of free energy. The second, the microscopic source, is derived from the energy released when the initial velocity distribution relaxes toward thermal equilibrium.

This model does not include bounded magnetically confined laboratory plasmas, but places special emphasis on the importance of the plasma parameters such as Debye length, temperature, and mass, and their effect on the stability of the plasma. This approach will no doubt assist in the physical interpretation of instabilities as well as allowing the results to be extrapolated to more complicated cases.

Basically there are two mathematical models to describe a plasma, the hydrodynamic and kinetic formulations. Since the hydrodynamic equations are in reality velocity moments derived from the kinetic equations, they do not describe the detailed behaviour of the gas but only the macroscopic phenomena occurring in the plasma. The kinetic formulations, however, are able to account for the microscopic fluctuations as well. Landau damping was first discovered¹ using one of the basic kinetic equations, the collisionless Boltzmann equation. This

equation together with Maxwell's equations will also be the mathematical basis for this thesis.

The literature involving the combination of microscopic and macroscopic phenomena in plasmas, for the type of model described above has mainly dealt with the cases in which a distribution in random velocity is assumed in combination with at most two streams. Macroscopic phenomena for the same model, have, however been dealt with for the multi-stream case. In this regard, James and Vermeulen³ assumed a distribution in drift velocity in studying macroscopic phenomena in a microparticle plasma. This thesis will therefore try to bridge this gap in the literature, studying both microscopic and macroscopic phenomena using the collisionless Boltzmann equation.

Chapter 2

DERIVATION OF THE DISPERSION RELATION

2.1 Basic Equations

Various derivations of the dispersion relation for longitudinal and transverse waves in a warm plasma are given in Schmidt⁴, Bernstein⁵ and Tanenbaum⁶. The present treatment will make a brief review of the derivation of the dispersion relation. This will allow the introduction of all the important parameters and will show the limitations involved. Since the type of plasma to be considered is a multi-component gas, each component with its own given density, temperature, mass and streaming velocity, the Boltzmann equation for each component is:

$$\frac{\partial f_{\sigma}}{\partial t} + \vec{\nabla} \cdot \nabla_{\mathbf{r}} f_{\sigma} - \frac{q_{\sigma}}{m_{\sigma}} \left(\left(\vec{E} + \vec{v} \times \vec{B} \right) \cdot \nabla_{\mathbf{v}} f_{\sigma} \right) = \left(\frac{\partial f_{\sigma}}{\partial t} \right)_c \quad (2.1.1)$$

where f_{σ} is the distribution of the σ component and is a function of position, velocity, and time.

Here q_{σ} is the electric charge and m_{σ} is the mass of particles of the σ species and \mathbf{v} is the velocity, \mathbf{E} the total electric field, \mathbf{B} the total magnetic field,

$\left(\frac{\partial f_{\sigma}}{\partial t} \right)_c$ is the collision term.

Equation (2.1.1) together with Maxwell's equations, given below in MKS units, form a self-consistent set of equations.

$$\nabla \cdot \vec{E} = \frac{\rho(\vec{r}, t)}{\epsilon_0} = \sum_{\sigma} \frac{q_{\sigma}}{\epsilon_0} \int_{-\infty}^{\infty} f_{\sigma} d^3 v \quad (2.1.2)$$

where $\rho(\vec{r}, t)$ is the charge density and ϵ_0 the permittivity of free space.

Also,

$$\nabla \cdot \vec{B} = 0 \quad (2.1.3)$$

$$\nabla \times \vec{E} = - \frac{\partial \vec{B}}{\partial t} \quad (2.1.4)$$

$$\begin{aligned} c^2 (\nabla \times \vec{B}) &= \frac{\vec{J}(\vec{r}, t)}{\epsilon_0} + \frac{\partial \vec{E}}{\partial t} \\ &= \sum_{\sigma} \frac{q_{\sigma}}{\epsilon_0} \int_{-\infty}^{\infty} \vec{v} f_{\sigma} d^3 \vec{v} + \frac{\partial \vec{E}}{\partial t} \end{aligned} \quad (2.1.5)$$

Where $\vec{J}(\vec{r}, t)$ is the current density and c the velocity of light.

The distribution function will be represented by

$$f_{\sigma} = f_{0\sigma} + f_{1\sigma} e^{i\vec{k} \cdot \vec{x} - i\omega t} \quad (2.1.6)$$

Where $f_{0\sigma}$ is the equilibrium velocity distribution of each species and only velocity dependent and $f_{1\sigma}$ is the perturbed velocity distribution of each species. The assumption that $f_{0\sigma} \gg f_{1\sigma}$ will be made, since only linear interactions will be considered. Also, in equilibrium it will be assumed that space charge neutrality holds.

Because there are no external electric and magnetic fields, these will be treated as first order quantities:

$$\begin{aligned}\vec{E} &= \vec{E}_1 e^{i\vec{k} \cdot \vec{r} - i\omega t} & \text{and} \\ \vec{B} &= \vec{B}_1 e^{i\vec{k} \cdot \vec{r} - i\omega t}\end{aligned}\tag{2.1.7}$$

By substituting 2.1.6 and 2.1.7 into 2.1.1 to 2.1.5, the resulting first order equations are:

$$\begin{aligned}& \frac{\partial f_{1\sigma}}{\partial t} e^{i\vec{k} \cdot \vec{r} - i\omega t} + \vec{v} \cdot \nabla_r f_{1\sigma} e^{i\vec{k} \cdot \vec{r} - i\omega t} \\ & - \frac{q_\sigma}{m_\sigma} \left(\vec{E}_1 e^{i\vec{k} \cdot \vec{r} - i\omega t} + \vec{v} \times \vec{B}_1 e^{i\vec{k} \cdot \vec{r} - i\omega t} \right) \cdot \nabla_v f_{0\sigma} \\ & = \left(\frac{\partial f_\sigma}{\partial t} \right)_c \quad \text{at } f_\sigma = f_{0\sigma} + f_{1\sigma}\end{aligned}\tag{2.1.8}$$

$$i\vec{k} \cdot \vec{E}_1 = \sum_\sigma \frac{q_\sigma}{\epsilon_0} \int_{-\infty}^{\infty} f_{1\sigma} e^{i\vec{k} \cdot \vec{r} - i\omega t} d^3v\tag{2.1.9}$$

$$\vec{k} \cdot \vec{B}_1 = 0 \quad (2.1.10)$$

$$\vec{k} \times \vec{E}_1 = -i\omega \vec{B}_1 \quad (2.1.11)$$

and

$$c^2(\vec{k} \times \vec{B}_1) = \sum_{\sigma} \frac{q_{\sigma}}{\epsilon_0} \int_{-\infty}^{\infty} \vec{v} f_{1\sigma} e^{i\vec{k} \cdot \vec{r} - i\omega t} d^3v - i\omega \vec{E}_1 \quad (2.1.12)$$

Before the solution to the above equations is attempted, the collision term appearing in (2.1.1) and the zeroth order distribution function will be examined.

2.2 The Velocity Distribution Function

Distinction should be made between an equilibrium distribution and the most probable velocity distribution of all the particles in the plasma. When equilibrium is achieved, the velocity distribution should no longer be changed by collisions, hence the collision term in equation 2.1.1 is then equal to zero. The most probable distribution function is the one for which the Hamiltonian is a minimum.

It is quite well known⁶ that for a monatomic gas with a given temperature, density and mean velocity, both the equilibrium and the

most probable velocity distribution is the Maxwellian:

$$f_{0\sigma}(\vec{v}) = \frac{n_{\sigma} e^{-\vec{c}_{\sigma}^2 / a_{\sigma}^2}}{\pi^{3/2} a_{\sigma}^3} \quad (2.2.1)$$

where

$$a_{\sigma} = \left(\frac{k_B T_{\sigma}}{m_{\sigma}} \right)^{1/2} \quad (2.2.2)$$

a_{σ} is the thermal velocity, k_B Boltzmann's constant and T_{σ} the temperature, n_{σ} is the density while $\vec{c}_{\sigma} = \vec{v} - \vec{u}_{\sigma}$ \vec{u}_{σ} is the drift velocity. In this thesis \vec{u}_{σ} will be assumed to be in the x direction. For the plasma model being considered, the Maxwellian distribution (equation 2.2.1), for each species is the most probable distribution function since the Hamiltonian is a minimum⁶. The plasma is not necessarily at equilibrium since this is dependent on the collision term. For example, if the Boltzmann collision integral⁶ is assumed, which is used for two body collisions, the range of interparticle force laws being short, the most probable distribution function (equation 2.2.1) is not the equilibrium one since the collision term does not vanish for long times. On the other hand, if the Krook collision model⁶ is assumed:

$$\left(\frac{\partial f_{\sigma}}{\partial t} \right)_C = \nu (f_{0\sigma} - f_{\sigma}) \quad (2.2.3)$$

Where ν^{-1} is a heuristic relaxation time, the collision term vanishes, for times longer than ν^{-1} . The Krook model (also called the B.G.K. due to Bhatnagar-Gross and Krook) has some serious physical limitations.⁶ For example, every average macroscopic value approaches equilibrium at the same rate ν^{-1} . Actually, in the collisions between particles of two different species the change in the lighter species' momentum is more pronounced than the change in the lighter species' kinetic energy, hence the equilibration time for the mean energy of the lighter species is much longer. Therefore this collision model is only valid in the limit when ν approaches zero for a multi-component plasma. The most probable distribution function as given by equation (2.2.1) is the equilibrium distribution function in the limit of a collisionless plasma. The analysis in this thesis will be restricted to the limit where the plasma approaches the collisionless state.

2.3 The Dispersion Relation

Returning to equations 2.1.8 to 2.1.12 and substituting 2.2.1 to 2.2.3 into them, gives after performing differentiations with respect to time and space:

$$-i\omega f_{1\sigma} + i\vec{v} \cdot \vec{k} f_{1\sigma} + \frac{q_{\sigma}}{m_{\sigma}} \left(\vec{E}_1 + \vec{v} \times \vec{B}_1 \right) \cdot \frac{2\vec{c}_{\sigma}}{a_{\sigma}^2} \left(\frac{n_{\sigma} e^{-c_{\sigma}^2/a_{\sigma}^2}}{\pi^{3/2} a_{\sigma}^3} \right) = \nu f_{1\sigma} \quad (2.3.1)$$

$$i\vec{k} \cdot \vec{E}_1 = \sum_{\sigma} \frac{q_{\sigma}}{\epsilon_0} \int_{-\infty}^{+\infty} f_{1\sigma} d^3v \quad (2.3.2)$$

$$i\vec{k} \cdot \vec{B}_1 = 0 \quad (2.3.3)$$

$$i\vec{k} \times \vec{E}_1 = i\omega \vec{B}_1 \quad (2.3.4)$$

$$ic^2(\vec{k} \times \vec{B}_1) = \sum_{\sigma} \frac{q_{\sigma}}{\epsilon_0} \int_{-\infty}^{+\infty} \vec{v} f_{1\sigma} d^3v - i\omega \vec{E}_1 \quad (2.3.5)$$

Solving equation (2.3.1) for $f_{1\sigma}$ gives:

$$f_{1\sigma} = \frac{i 2 q_{\sigma} n_{\sigma} e^{-c_{\sigma}^2/a_{\sigma}^2} \vec{c}_{\sigma} \cdot \left(\vec{E}_1 + \vec{u}_{\sigma} \times \vec{B}_1 \right)}{m_{\sigma} \pi^{3/2} a_{\sigma}^5 (i v + \omega - \vec{v} \cdot \vec{k})} \quad (2.3.6)$$

Solving equation (2.3.4) for B_1 yields:

$$\vec{B}_1 = \frac{\vec{k}}{\omega} \times \vec{E}_1 \quad (2.3.7)$$

Equations (2.3.6) and (2.3.7) are now substituted in equation (2.3.5) to obtain the dispersion relation:

$$\frac{ic^2}{\omega} \left(\vec{k} \times (\vec{k} \times \vec{E}_1) \right) = \sum_{\sigma} \frac{i 2 q_{\sigma}^2 n_{\sigma}}{\epsilon_0 m_{\sigma} \pi^{3/2} a_{\sigma}^5} \int_{-\infty}^{\infty} \frac{d^3v \vec{v} e^{-c_{\sigma}^2/a_{\sigma}^2}}{i v + \omega - \vec{v} \cdot \vec{k}} \left[\vec{c}_{\sigma} \cdot \left(\vec{E}_1 + \frac{(\vec{u}_{\sigma} \times \vec{k} \times \vec{E}_1)}{\omega} \right) \right] - i \omega \vec{E}_1 \quad (2.3.8)$$

The transverse and longitudinal oscillations are uncoupled if there is no external magnetic field, or inhomogeneities in density or temperature.⁴ Therefore longitudinal waves ($\vec{k} \parallel \vec{E}_1$) and transverse waves ($\vec{k} \perp \vec{E}_1$) will be considered separately. The perturbation will be taken in the x direction. Hence $\vec{k} = \vec{k}_x$. By noting that the left hand side of equation (2.3.8) has only a transverse component: $\frac{-ic^2 k^2 \vec{E}_t}{\omega}$,

and by dividing through by $i\omega$, the following relation can be obtained from equation (2.3.8):

$$\frac{-c^2 k^2 \vec{E}_{1t}}{\omega^2} + \vec{E}_1 = \frac{1}{\omega \pi^{3/2}} \sum_{\sigma} \frac{k_D^2}{a_{\sigma}^3} \left[\int_{-\infty}^{\infty} \frac{\vec{c}_{\sigma} \cdot \vec{E}_1 + \vec{u}_{\sigma} \times \frac{\vec{k} \times \vec{E}_1}{\omega}}{i v + \omega - \vec{v}_x \cdot \vec{k}} d v (\vec{v}) e^{-c_{\sigma}^2/a_{\sigma}^2} \right] \quad (2.3.9)$$

where

$$k_{D\sigma}^2 = \frac{2n_{\sigma} q_{\sigma}^2}{a_{\sigma}^2 m_{\sigma} \epsilon_0}, \text{ and from}$$

equation (2.2.2):

$$k_{D\sigma}^2 = \frac{q_{\sigma}^2 n_{\sigma}}{T_{\sigma} \epsilon_0 k_B} \quad (2.3.10)$$

$k_{D\sigma}$ is the debye number for each species, and is the reciprocal of the debye length and the components of \vec{c}_{σ} are defined by

$$\vec{c}_{\sigma} = c_x \vec{i}_x + c_y \vec{i}_y + c_z \vec{i}_z$$

2.4 Longitudinal Waves

The x-component of equation (2.3.9) yields:

$$E_x = \frac{1}{\omega\pi^{3/2}} \sum_{\sigma} \frac{k_{D\sigma}^2}{a_{\sigma}^3} \int_{-\infty}^{\infty} d^3v \frac{v_x e^{-c_{\sigma}^2/a_{\sigma}^2} \vec{c}_{\sigma} \cdot \vec{E}_1}{i v + \omega - v_x k} \quad (2.4.1)$$

where \vec{i}_x = unit vector in x-direction.

To evaluate the integral in equation (2.4.1), the quantity $\vec{c}_{\sigma} + \vec{u}_{\sigma}$ is substituted for \vec{v} . (see equation (2.2.1)). By performing the dot product as well, the following equation is obtained:

$$E_x = \frac{1}{\omega\pi^{3/2}} \sum_{\sigma} \frac{k_{D\sigma}^2}{a_{\sigma}^3} \int_{-\infty}^{\infty} d^3c_{\sigma} e^{-c_{\sigma}^2/a_{\sigma}^2} \frac{(c_x + u_{\sigma})(c_x E_x + c_y E_y + c_z E_z)}{i v + \omega - (c_x + u_{\sigma}) k} \quad (2.4.2)$$

Integrals of the form:

$$\int_{-\infty}^{\infty} \int_{-\infty}^{\infty} \int_{-\infty}^{\infty} \frac{dc_x dc_y dc_z e^{-c_{\sigma}^2/a_{\sigma}^2} (c_x + u_{\sigma}) c_j E_j}{i v + \omega - (c_x + u_{\sigma}) k}, \quad (2.4.3)$$

with $j = y$ and z are identically equal to zero because the integrand is odd with respect to the y and z co-ordinates.

Hence there are only two non-zero terms in equation (2.4.2).

By dividing through by E_x the following equation is obtained:

$$1 = \frac{1}{\omega \pi^{3/2}} \sum_{\sigma} \frac{k_{D\sigma}^2}{a_{\sigma}^3} \int_{-\infty}^{\infty} \frac{dc_x (c_x + u_{\sigma}) c_x e^{-c_x^2/a_{\sigma}^2}}{i\nu + \omega - (c_x + u_{\sigma}) k} \times$$

$$\times \int_{-\infty}^{\infty} dc_y e^{-c_y^2/a_{\sigma}^2} \int_{-\infty}^{\infty} dc_z e^{-c_z^2/a_{\sigma}^2} \quad (2.4.4)$$

Notice that only the streaming in the x direction contributes to longitudinal waves, and that the second and third integrals are each equal to $\pi^{1/2} a_{\sigma}$.

The quantity z_{σ} is set equal to $\frac{i\nu + \omega - u_{\sigma} k}{a_{\sigma} k}$

In the limit of a collisionless plasma

$$z_{\sigma} = \frac{\omega - u_{\sigma} k}{a_{\sigma} k} \quad (2.4.5)$$

If p is defined from $c_x = p a_{\sigma}$, equation (2.4.4) now becomes:

$$1 = \frac{1}{\omega \pi^{1/2}} \sum_{\sigma} \frac{k_{D\sigma}^2}{k} \int_{-\infty}^{\infty} \frac{dp (p a_{\sigma} + u_{\sigma}) p e^{-p^2}}{z_{\sigma} - p} \quad (2.4.6)$$

If both the numerator and the denominator of the integrand in equation (2.4.6) are multiplied by $-(p+z_{\sigma})$ and if it is noted that the integral over all odd functions of p vanishes, the following is obtained:

$$1 = - \frac{1}{\pi^{\frac{1}{2}}} \sum_{\sigma} \frac{k_{D\sigma}^2}{k^2} \int_{-\infty}^{\infty} \frac{p^2 e^{-p^2} dp}{p^2 - z_{\sigma}^2} \quad (2.4.7)$$

Since

$$\frac{p^2}{p^2 - z_{\sigma}^2} = 1 + \frac{z_{\sigma}^2}{p^2 - z_{\sigma}^2} ,$$

equation (2.4.7) may be written as:

$$1 = - \sum_{\sigma} \frac{k_{D\sigma}^2}{k^2} \left(1 + z_{\sigma} \int_{-\infty}^{\infty} \frac{z_{\sigma} e^{-p^2} dp}{\pi^{\frac{1}{2}} (p^2 - z_{\sigma}^2)} \right) \quad (2.4.8)$$

The integral can be simplified in the following manner. The function $G(s)^6$ is introduced with:

$$G(s) = \frac{z_{\sigma}}{\pi^{\frac{1}{2}}} \int_{-\infty}^{\infty} \frac{e^{-sp^2} dp}{p^2 - z_{\sigma}^2} \quad (2.4.9)$$

$$\begin{aligned} \text{Now, } \frac{dG(s)}{ds} &= - \frac{z_{\sigma}}{\pi^{\frac{1}{2}}} \int_{-\infty}^{\infty} \frac{p^2 e^{-sp^2} dp}{p^2 - z_{\sigma}^2} \\ &= - \frac{z_{\sigma}}{\pi^{\frac{1}{2}}} \int_{-\infty}^{\infty} dpe^{-sp^2} \left(1 + \frac{z_{\sigma}^2}{p^2 - z_{\sigma}^2} \right) \end{aligned}$$

$$\text{Hence } \frac{dG(s)}{ds} = -z_\sigma s^{-1/2} - z_\sigma^2 G(s) \quad (2.4.10)$$

By multiplying equation (2.4.10) by $e^{sz_\sigma^2}$ and integrating from $s=0$ to $s=1$, the following is obtained:

$$\int_0^1 \frac{d}{ds} (G(s) e^{sz_\sigma^2}) ds = -z_\sigma \int_0^1 ds s^{-1/2} e^{sz_\sigma^2}$$

which is equal to:

$$G(1) e^{z_\sigma^2} - G(0) = -z_\sigma \int_0^1 ds s^{-1/2} e^{sz_\sigma^2} \quad (2.4.11)$$

A change of variable from s to $\frac{r^2}{z_\sigma^2}$

transforms equation (2.4.11) to

$$G(1) e^{z_\sigma^2} - G(0) = - \int_0^{z_\sigma} 2e^{r^2} dr \quad (2.4.12)$$

$$\text{Now from equation (2.4.9) } G(0) = \frac{z_\sigma}{\pi^{1/2}} \int_{-\infty}^{\infty} \frac{dp}{p^2 - z_\sigma^2} \quad (2.4.13)$$

Since z is complex, the poles $p = \pm z_\sigma$ are located anywhere in the complex plane. For every z_σ , one pole p is below and one is above the real axis. Therefore the theory of residues may be used to show that

$$G(0) = \pi^{\frac{1}{2}} i$$

In arriving at this result, the first part of the path of integration is chosen along the real axis, and the second part is chosen along the contour formed by a semi-circle about the upper half plane.

Hence, solving equation (2.4.12) for $G(1)$:

$$G(1) = -2 \int_0^{z_\sigma} e^{r^2 - z_\sigma^2} dr + i\pi^{\frac{1}{2}} e^{-z_\sigma^2} \quad (2.4.14)$$

$G(1)$ is a function of z_σ and is renamed $Z(z_\sigma)$. Hence

$$Z(z_\sigma) = -2 \int_0^{z_\sigma} e^{r^2 - z_\sigma^2} dr + i\pi^{\frac{1}{2}} e^{-z_\sigma^2} \quad (2.4.15)$$

By going back to equation (2.4.8) the dispersion relation for longitudinal waves may now be put in terms of $Z(z_\sigma)$ and so

$$k^2 = - \sum_{\sigma} k_{D\sigma}^2 (1 + z_\sigma Z(z_\sigma)) \quad (2.4.16)$$

2.5 Transverse Waves

The transverse component of equation (2.3.9) gives the following relation

$$-\frac{c^2 k^2}{\omega^2} \vec{E}_{1t} + \vec{E}_{1t} = \frac{1}{\omega \pi^{3/2}} \sum_{\sigma} \frac{k_{D\sigma}^2}{a_\sigma^3} \int \left[\frac{d^3 c_\sigma \bar{v}_t e^{-c_\sigma^2/a_\sigma^2}}{i\nu + \omega - \vec{v}_x \cdot \vec{k}_x} \times \right. \\ \left. \vec{c}_\sigma \cdot (\vec{E}_t + \vec{u}_\sigma \times \frac{\vec{k}_x \vec{E}_t}{\omega}) \right] \quad (2.5.1)$$

Since $E_x = 0$ for transverse waves and u_σ is in the x direction, equation (2.5.1) may be written for the y component:

$$-\frac{c^2 k^2}{\omega^2} + 1 = \frac{1}{\omega \pi^{3/2}} \sum_{\sigma} \frac{k_{D\sigma}^2}{a_{\sigma}^3} \int_{-\infty}^{\infty} dc_y c_y^2 e^{-c_y^2/a_{\sigma}^2} \times \\ \times \int_{-\infty}^{\infty} dc_z e^{-c_z^2/a_{\sigma}^2} \int_{-\infty}^{\infty} \frac{dc_x e^{-c_x^2/a_{\sigma}^2}}{\omega - c_x k_x + u_{\sigma} k_x} (1 - u_{\sigma} \frac{k_x}{\omega}) \quad (2.5.2)$$

A similar equation for the z component exists.

Moreover

$$-\frac{c^2 k^2}{\omega^2} + 1 = \frac{1}{\omega^2} \sum_{\sigma} \frac{k_{D\sigma}^2 a_{\sigma}^2}{2\pi^{1/2}} \int_{-\infty}^{\infty} \frac{dp e^{-p^2} z_{\sigma}}{z_{\sigma} - p} \quad (2.5.3)$$

In arriving at these expressions (equations (2.5.2) and (2.5.3)) an analysis similar to that in Section 2.4 is used.

By multiplying the integrand in equation (2.5.3) by $-(p+z_{\sigma})/-(p+z_{\sigma})$, this equation becomes:

$$\omega^2 - c^2 k^2 = -\frac{1}{2} \sum_{\sigma} k_{D\sigma}^2 a_{\sigma}^2 z_{\sigma} \int_{-\infty}^{\infty} \frac{z_{\sigma} e^{-p^2} dp}{\pi^{1/2} (p^2 - z_{\sigma}^2)} \quad (2.5.4)$$

which, in terms of $Z(z_{\sigma})$ is :

$$\omega^2 - c^2 k^2 = -\frac{1}{2} \sum_{\sigma} k_{D\sigma}^2 a_{\sigma}^2 Z(z_{\sigma}) z_{\sigma} \quad (2.5.5)$$

It will be convenient to replace ω/k by V_{ph} . Since V_{ph} is complex, it will be called 'complex phase velocity' in this thesis.

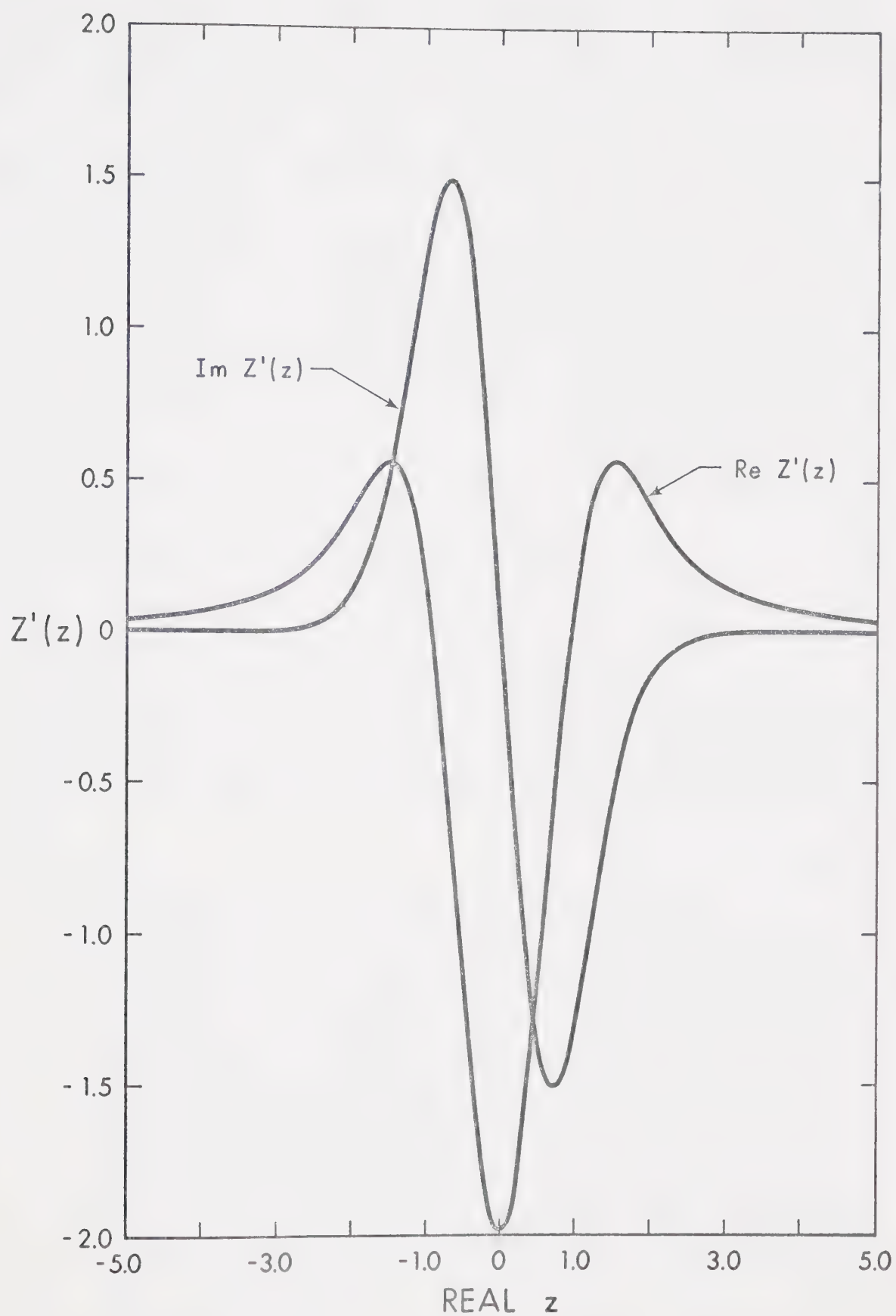


Figure 1.2 $Z'(z)$ for real z between -5 and +5

Hence equation (2.5.5) becomes:

$$k^2 = \frac{1}{2(c^2 - v_{ph}^2)} \sum_{\sigma} k_{D\sigma}^2 a_{\sigma}^2 Z(z_{\sigma}) z_{\sigma} \quad (2.5.6)$$

2.6 Qualitative discussion of the Dispersion Relations

The solution of equations (2.4.16) and (2.5.6.) is difficult without some knowledge of the behaviour of $Z(z_{\sigma})$. This function has been tabulated by Fried and Conte.⁷ By using the relationship⁷

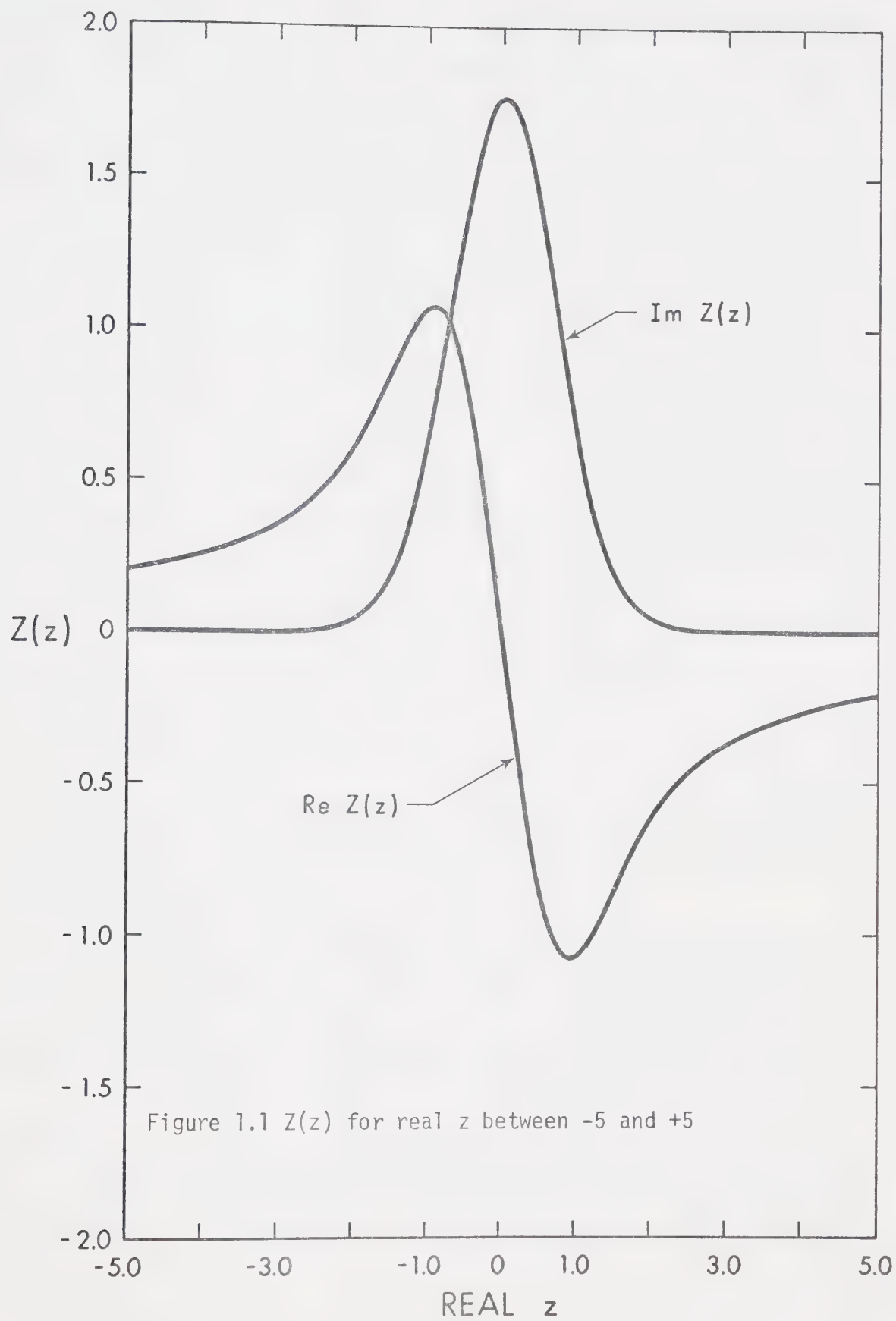
$$Z'(z_{\sigma}) = -2(1 + z_{\sigma} Z(z_{\sigma})), \quad (2.6.1)$$

equation (2.4.16) may be expressed as follows:

$$k^2 = \frac{1}{2} \sum_{\sigma} k_{D\sigma}^2 Z'(z_{\sigma}) \quad (2.6.2)$$

Only instabilities where k is real are examined (universal instabilities). The method of solution of equations (2.6.2) and (2.5.6) (in this thesis referred to as 'method A'), as outlined by Tanenbaum⁶ is straightforward:

1. A suitable complex phase velocity ω/k is chosen.
2. z_{σ} , one for each component is found from equation (2.4.5).
3. k is found from equation (2.6.2) for longitudinal waves and from equation (2.5.6) for transverse waves.
4. Since k is now known, ω can be found from the value of the phase velocity assumed in step 1.
5. By trial and error, values for ω/k can be obtained such that k is real. If the imaginary part of ω is found to be positive, the solution is unstable, while a negative imaginary implies a stable solution.



From step 5 above, it follows that all complex phase velocities which result in unstable solutions lie in the upper half V_{ph} plane. Since the sign of the imaginary part of V_{ph} is the same as the sign of the imaginary part of z_σ , the poles z_σ of the integrals in (2.4.6) and (2.5.4) also will lie in the upper half z_σ plane when unstable solutions exist. Conversely stable solutions correspond to values of V_{ph} and z_σ in the lower half of the V_{ph} and z_σ planes respectively.

Since the pole z_σ corresponds to the σ th stream in the plasma, there will be as many poles z_σ as there are streams for each V_{ph} . The location of each pole z_σ in the z_σ plane is a function of the V_{ph} of the disturbance, and of the streaming and thermal velocity of the σ th stream as can be seen from equation (2.4.5). For every case considered in this thesis, a reference frame will be chosen such that the stream with the lowest drift velocity (called the first stream $\sigma=1$) has $u_1=0$.

Consequently

$$z_1 = \frac{V_{ph}}{a_1} \quad (2.6.3)$$

so that z_1 will always lie in the same quadrant in the complex plane as the V_{ph} of the disturbance.

Every pole z_σ will contribute a real part, $k_{D\sigma}^2 (\text{Re } Z(z_\sigma))$ or $k_{D\sigma}^2 (\text{Re } Z'(z_\sigma))$, to the dispersion relations and an imaginary part $k_{D\sigma}^2 (\text{Im } Z(z_\sigma))$ or $k_{D\sigma}^2 (\text{Im } Z'(z_\sigma))$. For k to be real, k^2 must be positive and real.

Since k^2 is directly proportional to $Z(z_\sigma)$ or $Z'(z_\sigma)$, the location of the pole z_σ in the z_σ plane largely determines the effect of the σ th

stream on the stability of the plasma.

The real and imaginary parts of the functions $Z(z_\sigma)$ and $Z'(z_\sigma)$ have at most 3 maxima or minima and are always finite for constant imaginary z_σ in the upper half plane, as can be seen from the tables given by Fried and Conte⁷. As $|z_\sigma|$ increases the humps are much less pronounced. On the other hand, when z_σ is in the lower half plane, the functions oscillate rapidly for $|z_{\text{imag}}| \gtrsim |z_{\text{real}}|$ ⁷. The peak amplitudes approach infinity as $|z_{\text{imag}}|$ increases for constant z_{real} .

In the lower half plane because of the many zeroes of $\text{Im } Z(z_\sigma)$ and $\text{Im } Z'(z_\sigma)$, there are over 50 zero's for constant $\text{imag}(z_\sigma)=-9$, there will always be values of the complex phase velocity in the lower half V_{ph} plane for which k^2 is real and positive. Consequently, if no values of V_{ph} can be found in the upper half V_{ph} plane for which k^2 is real and positive, it may be concluded the plasma is stable.

For transverse waves, without solving equation (2.5.6) explicitly, it will now be shown that this model predicts that no instabilities exist for transverse waves, assuming $c \gg |V_{\text{ph}}|$. With this approximation, equation (2.5.6) becomes, using equation (2.6.1):

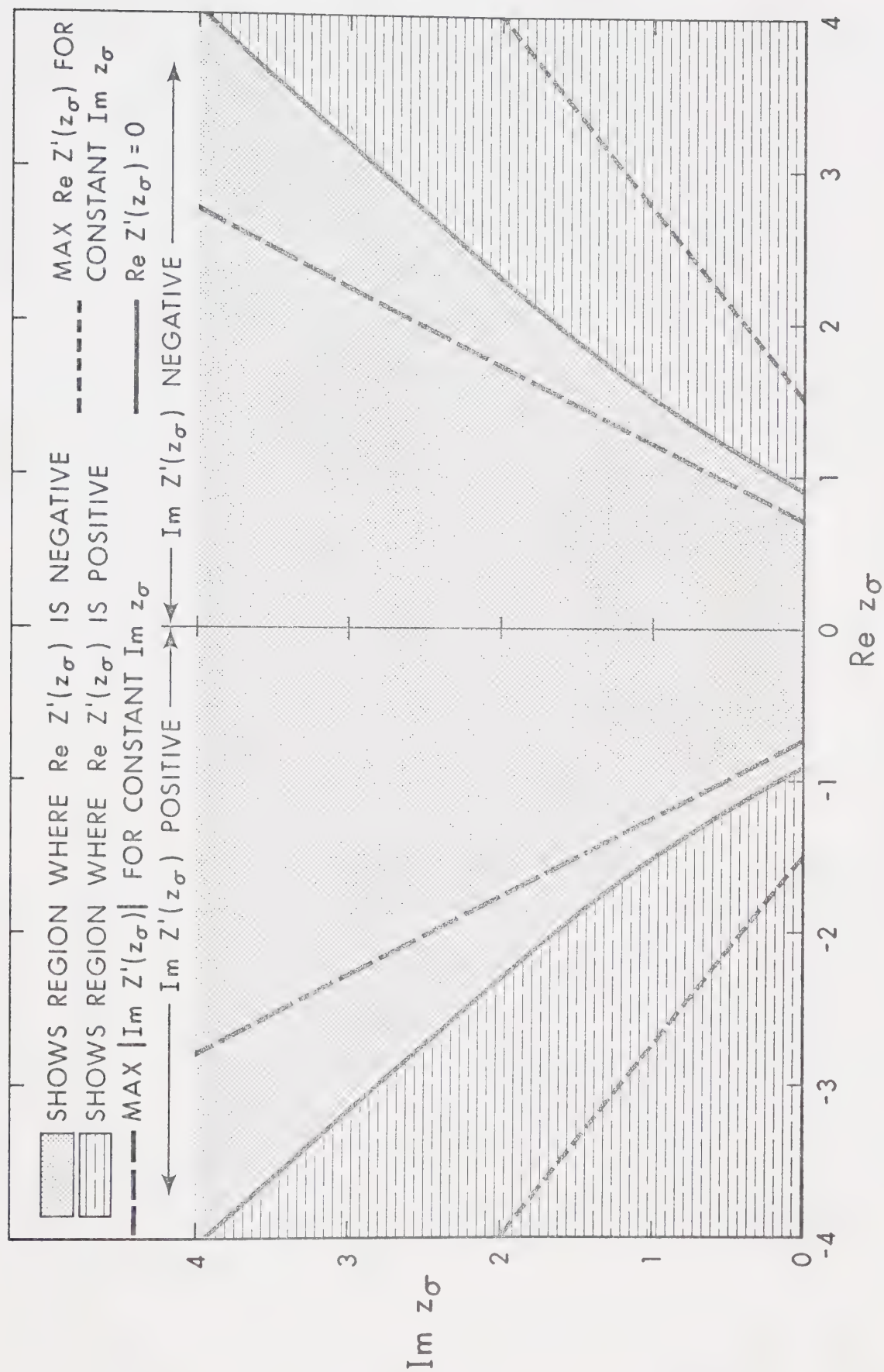
$$k^2 = -\frac{1}{4c^2} \sum_{\sigma} k_{D\sigma}^2 a_{\sigma}^2 (Z'(z_{\sigma}) + 2) \quad (2.6.4)$$

When solutions exist, $\text{Re}(k^2) \geq 0$ and for unstable solutions, $\text{Im}(V_{\text{ph}}) > 0$.

However, the right hand side of equation (2.6.4) is always negative since $\text{Re } Z'(z_{\sigma}) > -2$ for $\text{Im}(V_{\text{ph}}) > 0$ from the tables of Fried and Conte⁷.

Since no values of $|V_{ph}| \ll c$ exist for which k^2 is real and positive when V_{ph} is in the upper half V_{ph} plane, this model predicts that transverse disturbances in plasmas are stable when $|V_{ph}| \ll c$. Under these restrictions, instabilities for transverse waves are possible, however, when velocity distributions are anisotropic² or when there is an applied magnetic field⁶. These cases will not be studied in this thesis.

The solution for longitudinal waves (equation 2.6.2) will now be considered in more detail.

Figure 2 Upper Half z_σ Plane

2.7 Effect of Parameters on Distribution Function

The upper half plane is given in Figure 2.

Region N is where $\text{Re}[Z'(z_\sigma)]$ is negative

Region P is where $\text{Re}[Z'(z_\sigma)]$ is positive

The right-hand plane is where $\text{Im}[Z'(z_\sigma)]$ is negative

The left-hand plane is where $\text{Im}[Z'(z_\sigma)]$ is positive

For unstable solutions to exist, there must exist at least two poles, not all of them in the same quadrant in the upper-half z_σ plane. Otherwise $\sum_{\sigma} k_{D\sigma}^2 \text{Im} Z'(z_\sigma) \neq 0$ and then $\text{Im}(k^2) \neq 0$ as can be seen from equation (2.6.2). At least one pole must lie in region P so that k^2 can be positive. Poles in region N will be referred to as stabilizing and poles in region P as unstabilizing.

By using equation (2.4.5) the poles z_σ may be expressed in terms of V_{ph} as follows:

$$z_n = \frac{V_{ph} - u_n}{a_n} \quad (2.7.1)$$

To test for instability, given all parameters ($k_{D\sigma}^2$, a_σ , u_σ) of each stream in the plasma, every possible point V_{ph} in the upper V_{ph} plane must be checked until solutions are found by method A in Section 2.6. As can be seen from Fried and Conte⁷, $\text{Re } Z'(z_\sigma)$ is even and $\text{Im} Z'(z_\sigma)$ is odd for constant $\text{Im}(z_\sigma)$. A reference frame such that $u_1=0$ and $u_2, u_3 \dots \geq 0$ is chosen. Then for any V_{ph} chosen in the upper left-hand V_{ph} plane, the z_σ 's also lie in the upper left-hand z_σ plane and so no instabilities exists. Hence V_{ph} need only be considered in the upper right-hand V_{ph} plane.

The choice of V_{ph} can be restricted even further by the following method. The largest magnitude in streaming velocity will be denoted by u_m . Then only the $\text{Re}(V_{ph}) < u_m$ need be considered, since for $\text{Re}(V_{ph}) \geq u_m$ all poles z_σ lie in the right-hand z_σ plane and no unstable solutions can exist, as explained earlier. According to the tables of Fried and Conte⁷, if $\text{Im}(z_\sigma) \geq |\text{Re}(z_\sigma)|$, the pole z_σ will lie in region N. Hence from equation (2.7.1), if $\text{Im}(V_{ph}) > u_m$ all poles z_σ will lie in region N. In summary, only V_{ph} such that $\text{Re}(V_{ph}) < u_m$ and $\text{Im}(V_{ph}) < u_m$ need be checked in the upper right-hand plane for unstable solutions.

It will now be shown, that, for constant $\text{Im}(V_{ph})$, there will be at least one $\text{Re}(V_{ph})$ for which $\text{Im}(k^2) = 0$. A reference frame is chosen such that $u_1=0$ and $u_2, u_3 \dots \geq 0$ as above. If there is at least one stream i such that $u_i > 0$, when $\text{Re}(V_{ph}) = 0$, $\sum_\sigma k_{D\sigma}^2 \text{Im}[Z'(z_\sigma)] > 0$ as can be seen from Figure 2. Moreover, when $\text{Re}(V_{ph}) = u_m$, $\sum_\sigma k_{D\sigma}^2 \text{Im}[Z'(z_\sigma)] < 0$. Hence, for any given $\text{Im}(V_{ph})$, there will be at least one V_{ph} such that $\sum_\sigma k_{D\sigma}^2 \text{Im}[Z'(z_\sigma)] = 0$ and this V_{ph} will be denoted by $(V_{ph})_s$. If and only if $\sum_\sigma k_{D\sigma}^2 \text{Re}[Z'(z_\sigma)] \geq 0$ at $V_{ph} = (V_{ph})_s$, will there be a solution.

Next it will be shown that, if there exists a solution, there will be at least one V_{ph} ($=V_0$) for which $\sum_\sigma k_{D\sigma}^2 \text{Re}[Z'(z_\sigma)] = 0$. When there exists a solution, $\sum_\sigma k_{D\sigma}^2 \text{Re}[Z'(z_\sigma)] > 0$ for $\text{Im}(V_{ph}) < u_m$. When $\text{Im}(V_{ph}) = u_m$, all z_σ will lie in region N and so $\sum_\sigma k_{D\sigma}^2 \text{Re}[Z'(z_\sigma)] < 0$. Hence, if the plasma is unstable at any $0 < \text{Im}(V_{ph}) < u_m$ there will be at least one $(V_{ph})_s = V_0$ for which $\sum_\sigma k_{D\sigma}^2 \text{Re}[Z'(z_\sigma)] = 0$.

Consider any plasma where all the parameters u_σ , a_σ , $k_{D\sigma}^2$ have been chosen or determined except u_m . It will be shown that if u_m is chosen high enough, the plasma will be unstable.

Now, u_m is chosen such that:

$$\begin{aligned} u_m &\gg \operatorname{Re}(z_a) a_\sigma \quad (\text{all } \sigma) \\ u_m &\gg u_\sigma \quad (\sigma \neq m) \\ u_m &\gg a_\sigma \quad (\text{all } \sigma) \end{aligned} \quad (2.7.2)$$

where $\operatorname{Re}(z_a) \geq \frac{a_\sigma}{a_s} \operatorname{Re}(z_b)$ (all σ)

$$\operatorname{Re}(z_a) \geq \operatorname{Re}(z_b)$$

The subscript s refers to that component for which

$$u_m \gg u_s \geq u_\sigma \quad (\sigma \neq m, s)$$

From the graphs of Fried and Conte⁷, there exists a z_b such that $\operatorname{Re}[Z'(z_\sigma)]$ is positive for values of $|\operatorname{Re}(z_\sigma)| > |\operatorname{Re}(z_b)|$ for constant $\operatorname{Im}(z_\sigma)$ all σ .

$$\text{At } V_{ph} = z_a a_s + u_s \quad \text{and} \quad \operatorname{Re}(z_b) > 0,$$

$$\operatorname{Re}(z_s) = \frac{a_s \operatorname{Re}(z_a) + u_s - u_s}{a_s} = \operatorname{Re}(z_a) \quad (2.7.3)$$

$$\operatorname{Im}(z_s) = \operatorname{Im}(z_a) \quad (2.7.4)$$

$$\operatorname{Re}(z_m) = \frac{a_s \operatorname{Re}(z_a) + u_s - u_m}{a_m} \approx -\frac{u_m}{a_m} \quad (2.7.5)$$

The contribution to (2.6.2) from z_m is very small since both $\operatorname{Re}[Z'(z_\sigma)]$ and $\operatorname{Im}[Z'(z_\sigma)]$ are small.

Also,

$$\text{Im}(z_m) = \frac{a_s \text{Im}(z_a)}{a_m} \quad (2.7.6)$$

$$\text{Re}(z_\sigma) = \frac{a_s \text{Re}(z_a)}{a_\sigma} + \frac{u_s - u_\sigma}{a_\sigma} \quad (2.7.7)$$

$$\text{Im}(z_\sigma) = \frac{a_s}{a_\sigma} \text{Im}(z_a) \quad (2.7.8)$$

Hence all poles lie in region P, so that $\text{Re}(k^2) > 0$, and all poles other than z_m lie in the right hand plane so that $\text{Im}(k^2) < 0$.

Moreover at $V_{ph} = u_m + a_m \text{Re}(z_b) + a_m \text{Im}(z_b)$ and $\text{Re}(z_b) < 0$

$$\text{Re}(z_{\sigma,s}) = + \frac{a_m}{a_{\sigma,s}} \text{Re}(z_b) + \left(\frac{u_m - u_{\sigma,s}}{a_{\sigma,s}} \right) \quad (2.7.9)$$

Since $\text{Re}(z_{\sigma,s})$ is very large, it gives a negligible contribution.

$$\text{Im}(z_{\sigma,s}) = \text{Im } z_b \left(\frac{a_m}{a_{\sigma,s}} \right) \quad (2.7.10)$$

$$\text{Re}(z_m) = \frac{a_m}{a_m} \text{Re}(z_b) + \frac{u_m - u_m}{a_m} = \text{Re}(z_b) \quad (2.7.11)$$

$$\text{Im}(z_m) = \text{Im}(z_b) \quad (2.7.12)$$

Again all poles lie in region P so that $\text{Re}(k^2) > 0$. Since all poles except z_m give a negligible contribution, $\text{Im}(k^2) > 0$.

Since for one value of V_{ph} , $\text{Im}(k^2) < 0$, and for another value $\text{Im}(k^2) > 0$, there exists at least one value of V_{ph} such that $\text{Im}(k^2) = 0$ while $\text{Re}(u_m + z_b a_m) > \text{Re}(V_{ph}) > \text{Re}(u_s + z_a a_s)$ since u_m is so much higher.

For any of these values of V_{ph} , $\text{Re}(k^2) > 0$ since all the poles stayed in region P. This proves an instability exists if u_m is large enough.

u_{min} will be defined as the minimum u_m for which instabilities exist.

(u_{min} is not necessarily $\gg z_a a_\sigma$)

Any change in the parameters a_σ , $k_{D\sigma}^2$, u_σ , T_σ etc. which cause an increase in u_{min} will be referred to as stabilizing since the range over which u_m can vary for an unstable solution has been reduced.

Likewise any change in these parameters which cause a decrease in u_{min} will be referred to as unstabilizing.

The definitions of important and negligible poles will be explained next. In a plasma where the number of components is greater than two, some poles z_σ might give negligible contributions compared to others. For instance, this may happen when $|z_i| \gg |z_j|$ ($k_{Di}^2 \sim 0(k_{Dj}^2)$) in which case the contribution of z_j may be considered negligible. A pole z_i is called important when any change in a_i , k_{Di}^2 or u_i causes a marked increase or decrease in u_{min} . The terms important and negligible poles will be used in conjunction with the term stabilizing pole which may be used to describe a pole z_i when, $\text{Re}[Z'(z_i)] < 0$. As explained before, when $\text{Re}Z'(z_i) < 0$, z_i is in region N.

How the parameters u_σ , a_σ , $k_{D\sigma}^2$ and T_σ affect the position of the poles and the stability of the plasma will now be discussed. If u_m is increased, the range of $\text{Im}(V_{ph})$ and $\text{Re}(V_{ph})$ to be tested will be increased, resulting in a greater range for $\text{Im}(V_{ph})$ for which $\text{Re}(k^2) \geq 0$.

Usually this is an unstabilizing change.

If

$$a_i > \frac{u_m}{0.924}, \quad |\operatorname{Re}(z_i)| < 0.924$$

and consequently z_i will be stabilizing. On the other hand, if $a_j \ll u_m$, $|z_j|$ will be quite large for $|V_{ph} - u_j| \sim 0(u_m)$ and therefore makes a negligible contribution. For the small range where $|V_{ph} - u_j| \sim 0(a_j)$ the pole makes a significant contribution.

The Debye number squared ($k_{D\sigma}^2$) is an effective weighting factor. In the limit that k_{Di}^2 approaches zero, the pole z_i can only make a small contribution to k^2 . For the case in which k_{Di}^2 is increased such that

$$|\operatorname{Im}[k_{Di}^2 Z'(z_i)]| > \left| \sum_{\sigma \neq i} \operatorname{Im}[k_{D\sigma}^2 Z'(z_\sigma)] \right|$$

no solution exists.

For the case when the pole z_i lies in region N a solution is impossible provided k_{Di}^2 is large enough to ensure that $\sum_{\sigma} k_{D\sigma}^2 \operatorname{Re} Z'(z_\sigma) < 0$. Since u_{\min} is increased with a large enough increase in $k_{D\sigma}^2$, such an increase of $k_{D\sigma}^2$ is a stabilizing change. Hence an increase in the largest $k_{D\sigma}^2$ can usually be classified as a stabilizing change.

Mass, m_σ is inversely proportional to a_σ^2 and is independent of $k_{D\sigma}^2$. Density, n_σ and q_σ^2 are proportional to $k_{D\sigma}^2$ and independent of a_σ . Consequently, the deductions made when a_σ is varied also hold when \sqrt{m} is varied and similarly, the deductions made when $k_{D\sigma}^2$ is varied

also hold when n_σ and q_σ^2 are varied.

Temperature, on the other hand, is a function of both the thermal velocity and Debye number. The pole z_σ is inversely proportional to $(T_\sigma)^{\frac{1}{2}}$ and $k_{D\sigma}^2$ is inversely proportional to T_σ . If T_σ is increased from the initial temperature $T_{\sigma i}$ to a critical value $T_{\sigma c}$, such that $k_{D\sigma c}^2 \ll k_{D\sigma i}^2$ and such that $z_{\sigma c} \sim 0(0,0)$, the pole $z_{\sigma c}$ will give a stabilizing contribution, since it is in the region near the origin in Figure 2. But the weighting factor $k_{D\sigma c}^2$ will make the contribution from $z_{\sigma c}$ very small compared to the initial contribution. Hence, T_σ can be increased such that z_σ makes a negligible contribution. It will now be shown that for T_σ sufficiently small ($T_{\sigma s}$) the contribution to k^2 will always increase. $T_{\sigma s}$ is assumed sufficiently small so that $z_{\sigma s}$ will be sufficiently large that the approximation $Z'(z_{\sigma s}) = -\frac{1}{z_{\sigma s}}$ can be made. This is the asymptotic expansion for $Z'(z_{\sigma s})$ given by Fried and Conte⁷. The contribution of $z_{\sigma i}$ to k^2 is given by:

$$k_{D\sigma i}^2 [\text{Re}[Z'(z_{\sigma i})] + j \text{Im}[Z'(z_{\sigma i})]] \quad (2.7.13)$$

Now:

$$z_{\sigma s} = \frac{z_{\sigma i}}{b^{\frac{1}{2}}} \quad (2.7.14)$$

$$Z'(z_{\sigma s}) \approx -\frac{b^{\frac{1}{2}}}{z_{\sigma i}} \quad (2.7.15)$$

$$k_{D\sigma s}^2 = \frac{k_{D\sigma i}^2}{b} \quad (2.7.16)$$

$$\text{Where } b = \frac{T_{\sigma s}}{T_{\sigma i}} \quad (2.7.17)$$

The contribution to k^2 from the pole $z_{\sigma s}$ will then be, in terms of the initial contribution:

$$- \frac{k_{D\sigma i}^2}{b^{\frac{1}{2}} z_{\sigma i}} \quad (2.7.18)$$

Hence, for $T_{\sigma s}$ sufficiently small, which implies b small, the contribution from equation (2.7.18) will be greater than that from equation (2.7.13). Therefore, a large decrease in T_{σ} will make the pole z_{σ} more important.

Section 2.7 will now be summarized.

1. Increasing u_m increases instability.
2. Increasing the largest $k_{D\sigma}^2$ increases stability.
3. When $a_i > \frac{u_m}{0.924}$, it causes pole z_i to be stabilizing.
4. When $a_i \ll u_m$, it causes pole z_i to make a negligible contribution.
5. Increasing T_i by a large amount causes z_i to make a negligible contribution.
6. Decreasing T_i by a large amount causes z_i to make an important contribution.

The summary above describes the usual cases. The various physical

mechanisms responsible for these instabilities will be reviewed in section 2.8. Then, in Chapter 3, using section 2.7 and the analysis of some special cases with the aid of the computer, the regions dominated by the different physical mechanisms (bunching and Landau damping) responsible for most of the instabilities will be established.

2.8 Physical Interpretation Review

Balancing the energy lost by particles to that gained by the disturbing waves, and using the dispersion relations of various plasma models, the complex interactions can be understood in the following way⁶.

In a plasma composed of at least two streams, a mechanism called bunching occurs. The electric field of a random disturbance in one stream causes an acceleration of particles in the second stream and a fluctuation in their density. The particles can carry this disturbance back to the original starting point of the first stream if they have streaming motion. If this latter disturbance is in phase with the original one, the wave will grow, so that an instability occurs. Thus, assuming one component at rest, for every different streaming velocity u_0 , there exists a mode for which the disturbance is in phase with the original one. Since the original disturbance is random, the different modes corresponding to different beams must be added to give the total effect. If the nodes of one mode fall on the troughs of the other, destructive interference occurs, called phase mixing, lessening the bunching effect. If there are many streams, this phase mixing tends to dampen the original disturbance.

Another interaction between particles and waves already mentioned in section 1.1, involves particles travelling at the phase velocity of the disturbing wave in a warm plasma. If there are more particles travelling infinitesimally slower than the phase velocity than there are travelling infinitesimally faster, the wave will lose more energy than it will gain, and damping occurs. If the reverse is true, that is, the slope of the velocity distribution is positive at the phase velocity, the wave will absorb more energy from the interacting particles than it will lose and instability ensues. This type of damping is generally known as Landau damping while the instability is sometimes called inverse Landau damping.

Classically² bunching is considered to occur in cold plasmas, and Landau damping in hot plasmas. In Chapter 3 it will be shown where the regions of validity for each instability actually are.

Chapter 3

QUANTITATIVE DISCUSSION

3.1 General

In order to illustrate the various interactions described in 2.8, consider the following plasmas. A warm, one component plasma with velocity distribution given by the Maxwellian (see equation 2.2.1) will be called plasma A. Assuming Landau damping dominates, all waves will be damped since the slope of the velocity distribution is negative everywhere. Section 3.2 will consider this case in more detail.

The cold plasma approximation to plasma A can be described as follows: an infinite number of cold beams each with its own velocity, but each beam infinitesimally spread apart in velocity space such that the distribution of velocities is Maxwellian. If bunching is assumed to dominate, this plasma will be stable, since the infinite number of streaming velocities will suffer phase mixing, as explained in section 2.8.

As a third example consider a plasma composed of two hot streams, each stream like plasma A. If inverse Landau damping dominates, the plasma will be unstable because part of the slope of the velocity distribution is positive. However, section 3.3 will show that even

though the slope of the distribution function is positive for a range of values of the phase velocity, the dispersion equation (2.6.2) will not allow growing waves for this range. The physical explanation of Landau damping emphasizes only the few particles which are in resonance with the disturbing wave, while bunching tends to emphasize the collective process of many more particles in the plasma. The warm double-humped distribution function will serve as an example to illustrate this point in more detail in section 3.3.

As a last example, consider two cold streams far apart in velocity space. This plasma will experience bunching and be unstable as described in section 2.8.

A thorough investigation of the dispersion relation (equation 2.6.2) using the distribution function (2.2.1) will help to determine the regions of validity of bunching and inverse Landau damping.

3.2 The "One-Component" Plasma

For a one component plasma, ions forming a fixed background, there exists only one pole. From Fig. 2, for only one pole z_1 , $\text{Re}[Z'(z_1)] < 0$ when $\text{Im}[Z'(z_1)] = 0$. Hence only in the lower half plane of z_0 will there be any poles for which $\text{Im}[Z'(z_1)]$ is zero, and $\text{Re}[Z'(z_1)]$ positive as explained in Chapter 2. This is a stable configuration and all waves will be damped when the component has a Maxwellian velocity distribution. The problem has been solved and discussed in various ways and at various lengths in textbooks and

papers^{2,4,5,6}. For the least damped solution and for phase velocities greater than $2\frac{1}{2}$ to 3 times the thermal velocity, the damping factor is very close to⁹

$$\omega_i = \frac{-\pi^{\frac{1}{2}} \omega_p^4 e^{-\omega_p^2/k^2 a^2}}{k^3 a^3} \quad (3.2.1)$$

Where ω_i , the imaginary part of ω , is the damping factor and ω_p , the plasma frequency. In terms of the distribution function, given in equation (2.2.1), and after integration over the transverse velocity components, the damping factor (3.2.1) is proportional to

$$\frac{\omega_p^3 f'(\omega_p/k)}{n k^2} \quad (3.2.2)$$

That is, the damping factor is proportional to the slope of the distribution function in this case. Therefore, for one component plasmas Landau damping prevails for disturbances with high phase velocities. As can be seen from equation (3.2.1), for phase velocities greater than approximately three times the thermal velocities, the actual damping factor becomes very small. Because there are very few particles interacting with the wave, these plasma oscillations can be considered as free modes⁸. Hence, Landau damping is considered an exponentially small effect.

However, for phase velocities smaller than and of the order of the thermal velocity, the damping factor no longer is proportional to

the slope of the distribution function. In these regions, the damping factor is very large⁹. The region of validity of Landau damping, the interaction between the particles and the wave at the phase velocity, includes, therefore, those disturbances with $V_{ph} > 2.5a_1$. The large damping factor for $V_{ph} \lesssim 2.5a_1$ may be caused by the phase mixing of the disturbances associated with bunching. However, this can only be determined when an analysis of phase mixing for warm plasmas has been carried out, and at present, to the writer's knowledge such a study has not been made. Qualitatively any Maxwellian velocity distribution should exhibit phase mixing.

Because bunching is caused by density fluctuations, it depends on Debye length. Moreover, because of its dissipative effects, high thermal velocities will diminish bunching.

3.3 Two Stream Instability

The following study of the two stream instability will show the regions of validity of inverse Landau damping and bunching. These regions will be established by studying the distribution relation (equation 2.2.1). First, the marginal stability case ($I_m(V_{ph}) \approx 0$) will be investigated. If the two stream instability is in the regime of marginal inverse Landau damping, equal numbers of particles are travelling slightly slower and slightly faster than the V_{ph} velocity. Hence,

$$\sum_{\sigma=1}^2 f'_{\sigma}(V_{ph}) = 0 \quad (3.3.1)$$

Where $f_{\sigma}(V_{ph})$ is the one dimensional distribution function of the σ component of the plasma. If solutions can be found for which $\sum_{\sigma} f'_{\sigma}(V_{ph}) \neq 0$, these solutions will not be in the regime of marginal inverse Landau damping.

By substituting equation (2.4.15) into equation (2.4.16) the following dispersion relation is obtained

$$k^2 = - \sum_{\sigma=1}^2 k_{D\sigma}^2 \left[1 - 2 z_{\sigma} \int_0^{z_{\sigma}} e^{r^2 - z_{\sigma}^2} dr + i \pi^{\frac{1}{2}} z_{\sigma} e^{-z_{\sigma}^2} \right] \quad (3.3.2)$$

Since the poles are located close to the real axis, the real part of equation (3.3.2) is approximately given by the first two terms on the right hand side, and the imaginary part is given by the last term on the right hand side. The imaginary term can be expressed in terms of the distribution function (equation 2.2.1) and so,

$$k^2 = - \sum_{\sigma} k_{D\sigma}^2 \left[1 - 2 z_{\sigma} \int_0^{z_{\sigma}} e^{r^2 - z_{\sigma}^2} dr - \frac{i \pi f'_{\sigma}(V_{ph}) a_{\sigma}^2}{2 n_{\sigma}} \right] \quad (3.3.3)$$

where the transverse velocities have been integrated out of the three dimensional distribution function. Since $\text{Im}(k^2) = 0$ for solutions to exist, as explained in Method A of Section 2.6 and 2.7

$$\sum_{\sigma} \frac{k_{D\sigma}^2 \pi f'_{\sigma}(V_{ph}) a_{\sigma}^2}{2 n_{\sigma}} = 0$$

Using equation (2.3.10) this condition becomes:

$$\sum_{\sigma} \frac{q_{\sigma}^2 \pi f'_{\sigma}(V_{ph})}{m_{\sigma}} = 0 \quad (3.3.4)$$

From equation (3.3.4) it can be seen that there will be no solutions which lie in the regime of marginal inverse Landau damping (equation 3.3.1) except for equal charge squared, mass ratio of both streams. This is why in general an explanation different from Landau damping should be sought for the warm two stream marginal instability. In this regime bunching would appear to dominate.

The above might seem to imply that the regime for inverse Landau damping includes two streams with equal Debye length. However, by analyzing this case for complex V_{ph} , it will be shown that this case too, belongs to the regime where bunching is probably valid, rather than inverse Landau damping.

The cases which correspond to the regime of inverse Landau damping are those for which

$$\sum_{\sigma} f'_{\sigma}[\text{Re}(V_{ph})] > 0 \quad (3.3.5)$$

By using the dispersion relation (2.6.2) it will be shown that, even when

$$\sum_{\sigma} f'_{\sigma}[\text{Re}(V_{ph})] = 0 \quad (3.3.6)$$

instabilities may still exist.

For a two component plasma with equal Debye numbers and thermal velocities, the dispersion relation becomes:

$$\frac{2k^2}{k_D^2} = Z'(z_1) + Z'(z_2) \quad (3.3.7)$$

where k_D is the Debye number. The poles z_1 and z_2 are complex. The streaming velocity u_1 is set equal to zero, as done in section 2.7.

From equation (2.4.5):

$$\begin{aligned} z_1 &= \frac{\omega_r}{ka} + \frac{i\omega_i}{ka} \quad \text{and} \\ z_2 &= \frac{\omega_r}{ka} - \frac{u}{a} + \frac{i\omega_i}{ka} \end{aligned} \quad (3.3.8)$$

Where ω_r is the real part of the frequency, and subscripts have been dropped from a and u . ω_i must be positive for an unstable solution to exist. When $\text{Im}(z_\sigma)$ is fixed, the symmetry properties of $Z'(z_\sigma)$ are such that $\text{Im}[Z'(z_\sigma)]$ is an odd function of $\text{Re}(z_\sigma)$ and $\text{Re}[Z'(z_\sigma)]$ is an even function. Therefore, for the imaginary part of the right-hand side of equation (3.3.7) to disappear

$$\frac{\omega_r}{ka} = - \left(\frac{\omega_r}{ka} - \frac{u}{a} \right) \quad (3.3.9)$$

By solving for $\text{Re}(V_{ph}) = \frac{\omega_r}{k}$, equation (3.3.9) becomes:

$$\text{Re}(V_{ph}) = \frac{u}{2} \quad (3.3.10)$$

Using equation (2.2.1) and (3.3.10), the sum of the derivative of the distribution functions at the phase velocity gives

$$\begin{aligned}
 & c_1 e^{-c_1^2/a^2} + c_2 e^{-c_2^2/a^2} \\
 &= -\frac{u}{2} e^{-(-u/2a)^2} + \frac{u}{2} e^{-(u/2a)^2} = 0
 \end{aligned} \tag{3.3.11}$$

Equation (3.3.6) holds rather than equation (3.3.5) showing that this case is not in the regime of inverse Landau damping, but indicating it is in the regime of bunching.

Since it has been established that the two equal stream instability does not lie in the regime of inverse Landau damping, it may be assumed that most multicomponent plasmas are likewise not dominated by inverse Landau damping if they have instabilities.

It may also be assumed that disturbances with $(V_{ph} - u_m) > 3a_m$ will be damped because they are in the regime of classical Landau damping. Because of the above, efforts will be concentrated on parameters such as thermal and streaming velocity and Debye number.

The functional relationships between the streaming velocity, plasma frequency, and thermal velocity for the marginal two stream instability will now be discussed in more detail. Let the stream with the lowest k_D be denoted by i , the stream with the highest k_D by j . For each stream there exists one pole z_k , ($k=i,j$) where z_k is given by equation (2.7.1). Solving for V_{ph} in terms of z_i and substituting in the equation for z_j , the following expression is obtained:

$$a_i z_i - a_j z_j = u_j - u_i \quad (3.3.12)$$

Since $\text{Im}[Z'(z_\sigma)]$ is odd for constant $\text{Im}(z_\sigma)$, $\text{Re}(z_i)$ and $\text{Re}(z_j)$ must have opposite signs for $\text{Im}(k^2)$ to equal zero in equation (2.6.2).

Since $\text{Im}(a_i z_i) = \text{Im}V_{ph} = \text{Im}(a_j z_j)$, the imaginary terms in (3.3.12) cancel. Therefore equation (3.3.12) can be written as follows:

$$a_i z_s + a_j z_L = |u_j - u_i| \quad (3.3.13)$$

where $z_s = \text{Re}|z_i|$ and $z_L = \text{Re}|z_j|$.

The quantities a , u are determined by each stream while z_s and z_L are restricted to such quantities that $\text{Im}(k^2) = 0$ and $\text{Re}(k^2) \geq 0$ in equation (2.6.2). Figure 3 shows z_s as a function of z_L for various values of k_{Di}/k_{Dj} . This graph can be used to determine whether warm two stream plasmas are unstable or not. If z_s and z_L exist such that equation (3.3.13) holds, the plasma is unstable. The minimum relative difference streaming velocity required for instability can be determined by choosing the quantities z_s , z_L such that the slope of the z_s vs. z_L curve is equal to $-a_i/a_j$ from $\frac{d}{ds} |u_j - u_i| = 0$.

This section will be concluded by studying a multi-stream plasma which can be reduced to an equivalent two stream plasma.

In a research note Gautem¹⁰ et al report various machine calculations from the Saha equations to obtain realistic densities of the ionic species for given electron densities and temperature. The parameters given in that note will be used as an example for solving the

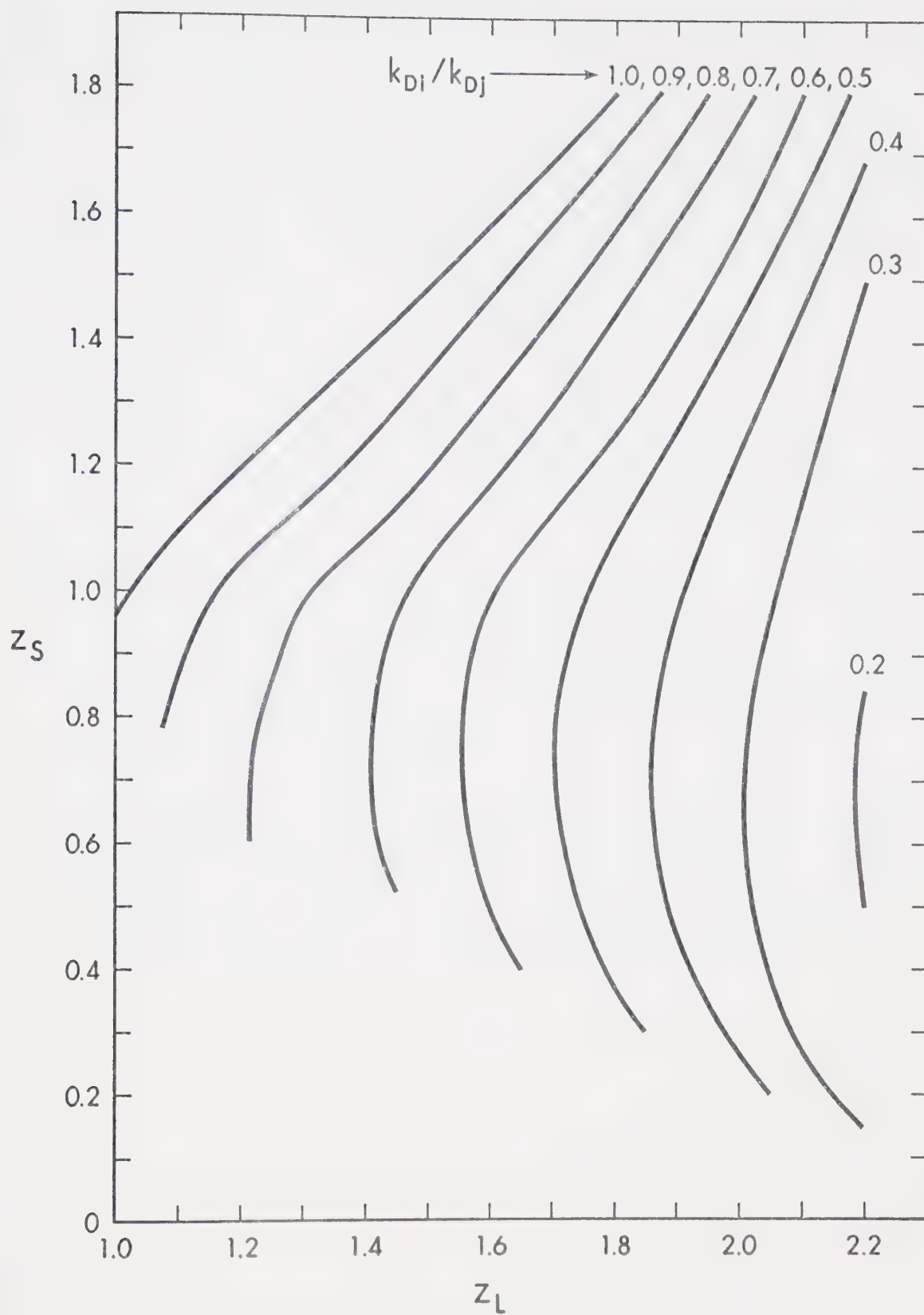


Figure 3 Values of z_L and z_S for various k_{Di}/k_{Dj}

dispersion relation (equation 2.6.2). The function $Z(z_\sigma)$ given in equation (2.4.15) was programmed on the I.B.M. 360 computer (see Appendix). By using method A as outlined in section 2.6, the onset of instability was determined by taking z_σ real for various values of the streaming velocity for each component. This again was programmed on the I.B.M. 360 computer. The various results obtained for the instability of this plasma are summarized in the following tables.

T refers to temperature

N refers to the number of ion and electron streams

U refers to the case when all the ions streams are at 'rest'

($U_{\text{ion}}=0$)

U1 refers to the case when only the first ion stream $\sigma=1$ is at

rest and all other ion streams are at U_e . Similarly U2 refers

to the case when only the second ion stream $\sigma=2$ is at rest and all other ion streams are at U_e .

The explanation of U3, U4, U5 and U6 are all similar to U1 and U2.

U_e refers to the minimum streaming velocity of the electron stream required for instability in any of the above mentioned cases.

TABLE 3.3.1 Instability of a Multi-Component Plasma

$\sigma =$	1	2	3	e
$T = 10,000$				
$N = 4$				
$k_{D\sigma}$	1.12×10^7	4.26×10^1	7.00×10^{-10}	1.12×10^7
a_σ	3.22×10^3	3.22×10^3	3.22×10^3	5.50×10^5

	U_e	U_e/a_e
U	4.82×10^5	0.875
U1	4.96×10^5	0.904
U2	3.30×10^6	6.00

TABLE 3.3.2 Instability of a Multi-Component Plasma

σ	1	2	3	4	e
T=15,000					
N=5					
$k_{D\sigma}$	9.17×10^6	3.98×10^4	3.48×10^{-2}	5.43×10^{-12}	$9.17 \times 10^{+6}$
a_σ	3.95×10^3	3.95×10^3	3.95×10^3	3.95×10^3	6.74×10^5

	U_e	U_e/a_e
U	6.05×10^5	0.900
U1	6.08×10^5	0.903
U2	2.43×10^6	3.60
U3	4.34×10^6	6.45

TABLE 3.3.3 Instability of a Multi-Component Plasma

σ	1	2	3	4	e
T=20,000					
N=5					
$k_{D\sigma}$	7.89×10^6	1.20×10^6	2.55×10^2	8.60×10^{-5}	7.94×10^6
a_σ	4.56×10^3	4.56×10^3	4.56×10^3	4.56×10^3	7.78×10^5

	U_e	U_e/a_e
U	7.02×10^5	0.909
U1	7.13×10^5	0.915
U2	1.83×10^6	2.36
U3	4.66×10^6	5.98
U4	5.69×10^6	7.30

TABLE 3.3.4 Instability of a Multi-Component Plasma

σ	1	2	3	4
T=25,000				
N=6				
$k_{D\sigma}$	5.22×10^6	6.81×10^6	4.08×10^4	1.43×10^0
a_σ	5.10×10^3	5.10×10^3	5.10×10^3	5.10×10^3

σ	5	e
T=25,000		
N=6		
$k_{D\sigma}$	6.98×10^{-9}	7.10×10^6
a_σ	5.10×10^3	8.70×10^5

	U_e	U_e/a_e
U	5.48×10^5	0.629
U1	1.15×10^6	1.32
U3	3.07×10^6	3.53
U4	5.22×10^6	6.00
U5	7.39×10^6	8.50

TABLE 3.3.5 Instability of a Multi-Component Plasma

σ	1	2	3	4
T=30,000				
N=7				
$k_{D\sigma}$	1.59×10^6	8.88×10^6	5.05×10^5	4.00×10^2
a_σ	5.58×10^3	5.58×10^3	5.58×10^3	5.58×10^3

σ	5	6	e
T=30,000			
N=7			
$k_{D\sigma}$	1.81×10^{-4}	8.11×10^{-13}	6.48×10^6
a_σ	5.58×10^3	5.58×10^3	9.53×10^5

	U_e	U_e/a_e
U	4.84×10^5	0.507
U1	2.01×10^6	2.11
U2	4.87×10^5	0.511
U3	2.51×10^6	2.64
U4	5.70×10^6	5.99
U5	6.84×10^6	7.20

TABLE 3.3.6 Instability of a Multi-Component Plasma

σ	1	2	3	4
T=35,000				
N=7				
$k_{D\sigma}$	5.14×10^5	8.23×10^6	2.38×10^6	1.78×10^4
a_σ	6.03×10^3	6.03×10^3	6.03×10^3	6.03×10^3

σ	5	6	e
T=35,000			
N=7			
$k_{D\sigma}$	2.09×10^{-1}	4.68×10^{-8}	6.00×10^6
a_σ	6.03×10^3	6.03×10^3	1.03×10^6

	U_e	U_e/a_e
U	4.74×10^5	0.460
U1	2.67×10^6	2.59
U2	5.27×10^5	0.514
U3	1.88×10^6	1.82
U4	3.83×10^6	3.72
U5	6.22×10^6	6.05
U6	8.49×10^6	8.24

TABLE 3.3.7 Instability of a Multi-Component Plasma

σ	1	2	3	4
T=40,000				
N=7				
$k_{D\sigma}$	1.73×10^5	6.14×10^6	6.15×10^6	2.49×10^5
a_σ	6.45×10^3	6.45×10^3	6.45×10^3	6.45×10^3

σ	5	6	e
T=40,000			
N=7			
$k_{D\sigma}$	3.42×10^1	1.45×10^{-4}	5.61×10^6
a_σ	6.45×10^3	6.45×10^3	1.10×10^6

	U_e	U_e/a_e
U	4.04×10^5	0.367
U1	3.29×10^6	2.97
U2	8.83×10^5	0.803
U4	3.14×10^6	2.86
U5	6.60×10^6	6.00
U6	7.9×10^6	7.20

TABLE 3.3.8 Instability of a Multi-Component Plasma

σ	1	2	3	4
T=45,000				
N=7				
$k_{D\sigma}$	4.68×10^4	3.11×10^6	8.27×10^6	1.26×10^6
a_σ	6.84×10^3	6.84×10^3	6.84×10^3	6.84×10^3

σ	5	6	e
T=45,000			
N=7			
$k_{D\sigma}$	1.18×10^3	4.94×10^{-2}	5.29×10^6
a_σ	6.84×10^3	6.84×10^3	1.17×10^6

	U_e	U_e/a_e
U	3.39×10^5	0.290
U1	3.97×10^6	3.40
U3	4.34×10^5	0.371
U4	2.48×10^6	2.12
U5	6.98×10^6	5.96
U6	7.36×10^6	6.30

TABLE 3.3.9 Instability of a Multi-Component Plasma

σ	1	2	3	4
T=50,000				
N=7				
$k_{D\sigma}$	1.25×10^4	1.36×10^6	7.97×10^6	3.52×10^6
a_σ	7.21×10^3	7.21×10^3	7.21×10^3	7.21×10^3

σ	5	6	e
T=50,000			
N=7			
$k_{D\sigma}$	1.56×10^4	4.08×10^0	5.02×10^6
a_σ	7.21×10^3	7.21×10^3	1.23×10^6

	U_e	U_e/a_e
U	2.98×10^5	0.242
U1	4.64×10^6	3.78
U3	4.58×10^5	0.373
U4	1.69×10^6	1.37
U5	4.56×10^6	3.71
U6	7.38×10^6	6.00

TABLE 3.3.10 Instability of a Multi-Component Plasma

σ	1	2	3	4
T=55,000				
N=7				
$k_{D\sigma}$	3.27×10^3	5.39×10^5	6.09×10^6	6.45×10^6
a_σ	7.56×10^3	7.56×10^3	7.56×10^3	7.56×10^3

σ	5	6	e
T=55,000			
N=7			
$k_{D\sigma}$	1.02×10^5	1.21×10^2	4.79×10^6
a_σ	7.56×10^3	7.56×10^3	1.29×10^6

	U_e	U_e/a_e
U	3.12×10^5	0.242
U1	5.30×10^6	4.10
U2	3.20×10^6	2.48
U3	7.23×10^5	0.560
U6	7.74×10^6	5.99

TABLE 3.3.11 Instability of a Multi-Component Plasma

σ	1	2	3	4
T=60,000				
N=7				
$k_{D\sigma}$	8.11×10^2	1.87×10^5	3.67×10^6	8.11×10^6
a_σ	7.90×10^3	7.90×10^3	7.90×10^3	7.90×10^3

σ	5	6	e
T=60,000			
N=7			
$k_{D\sigma}$	3.74×10^5	1.55×10^3	4.58×10^6
a_σ	7.90×10^3	7.90×10^3	1.35×10^6

	U_e	U_e/a_e
U	2.21×10^5	0.164
U1	5.98×10^6	4.44
U2	3.89×10^6	2.89
U4	3.19×10^5	0.236
U5	3.53×10^6	2.61
U6	5.77×10^6	4.27

TABLE 3.3.12 Instability of a Multi-Component Plasma

σ	1	2	3	4
T=65,000				
N=7				
$k_{D\sigma}$	2.13×10^2	6.49×10^4	2.04×10^6	8.44×10^6
a_σ	8.22×10^3	8.22×10^3	8.22×10^3	8.22×10^3

σ	5	6	e
T=65,000			
N=7			
$k_{D\sigma}$	9.65×10^5	1.16×10^4	4.40×10^6
a_σ	8.22×10^3	8.22×10^3	1.40×10^6

U	1.87×10^5	0.133
U1	6.63×10^6	4.75
U2	4.55×10^6	3.25
U3	2.40×10^6	1.71
U4	3.00×10^5	0.214
U5	3.04×10^6	2.17
U6	5.36×10^6	3.83

TABLE 3.3.13 Instability of a Multi-Component Plasma

σ	1	2	3	4
$T=70,000$				
$N=7$				
k_{Dr}	6.33×10^{-1}	1.44×10^{-4}	1.15×10^{-4}	8.18×10^{-6}
a_e	8.53×10^3	8.53×10^3	8.53×10^3	8.53×10^3

σ	5	6	e
$T=70,000$			
$N=7$			
k_{Dr}	2.05×10^{-6}	6.12×10^{-5}	4.24×10^{-6}
a_e	8.53×10^3	8.53×10^3	1.46×10^6

	U_e	U_e/a_e
U	1.94×10^{-5}	0.133
U1	8.73×10^{-6}	0.58
U4	2.75×10^{-5}	0.188
U5	2.46×10^{-6}	1.68

TABLE 3.3.14 Instability of a Multi-Component Plasma

σ	1	2	3	4
T=75,000				
N=7				
$k_{D\sigma}$	2.07×10^1	9.75×10^3	6.58×10^5	7.46×10^6
a_σ	8.83×10^3	8.83×10^3	8.83×10^3	8.83×10^3

σ	5	6	e
T=75,000			
N=7			
$k_{D\sigma}$	3.69×10^6	2.44×10^5	4.10×10^6
a_σ	8.83×10^3	8.83×10^3	1.51×10^6

	U_e	U_e/a_e
U	2.00×10^5	0.132
U1	9.02×10^6	5.98
U2	5.70×10^6	3.78
U3	3.49×10^6	2.31
U4	3.58×10^5	0.237
U6	4.14×10^6	2.67

TABLE 3.3.15 Instability of a Multi-Component Plasma

σ	1	2	3	4
T=80,000				
N=7				
$k_{D\sigma}$	6.92×10^0	3.89×10^3	3.59×10^5	6.15×10^6
a_σ	9.12×10^3	9.12×10^3	9.12×10^3	9.12×10^3

σ	5	6	e
T=80,000			
N=7			
$k_{D\sigma}$	5.54×10^6	7.36×10^5	3.97×10^6
a_σ	9.12×10^3	9.12×10^3	1.56×10^6

U	2.31×10^5	0.148
U1	9.34×10^6	5.98
U2	6.26×10^6	4.01
U4	5.80×10^5	0.372
U6	3.50×10^6	2.24

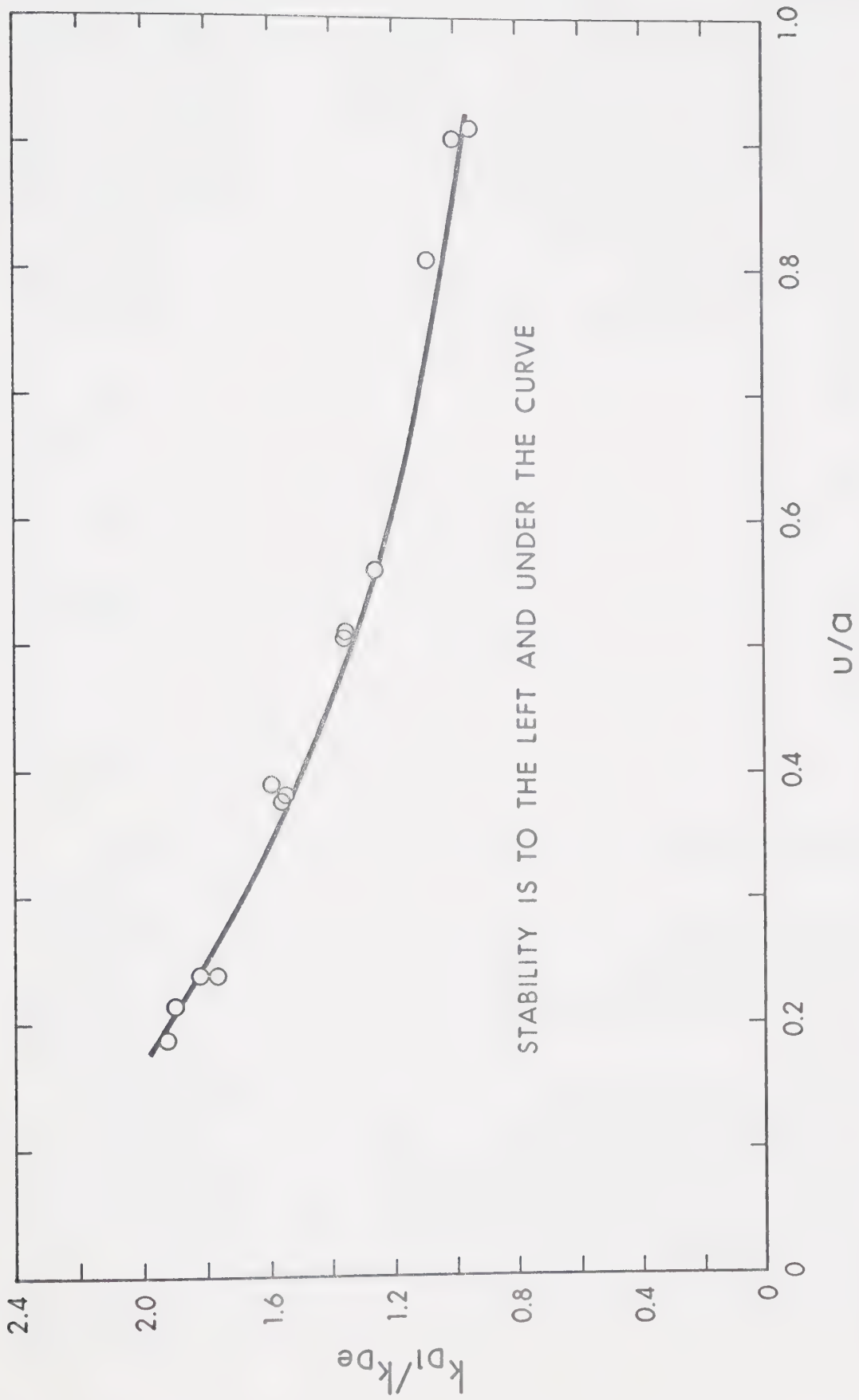


Figure 4 Marginal Stability

These results will be examined by reducing these cases to the two stream case.

When all the ion streams are at rest (case U), the dispersion relationship (equation 2.6.2) is the same as if there were only two streams, with thermal velocities \bar{a}_1 and \bar{a}_2 respectively and Debye number \bar{k}_{D1} and \bar{k}_{D2} respectively. In terms of the quantities from case U, these new thermal velocities and Debye numbers are:

$$\bar{a}_1 = a_{ion}$$

$$\bar{a}_2 = a_e$$

$$\bar{k}_{D1}^2 = \sum_{\sigma=1}^{N-1} k_{D\sigma}^2$$

$$\bar{k}_{D2} = k_{De}$$

Figure 4 shows the marginal instability for this case in terms of \bar{k}_{D1}/k_{De} vs U_e/a_e .

When only one ion stream is at rest (cases U1-U6) the dispersion relation can no longer be used to reduce this to the two stream case in the same way as was done with case U.

The thermal velocities of the ion streams at the same streaming velocity as the electron stream are not equal to the electron stream's thermal velocity. However, since the thermal velocities of the ion streams are much less than the minimum velocity required for instability (U_e), the ion streams which are not at rest may have a negligible effect

as was discussed in section 2.7. If we ignore those ion streams, the cases U1-U6 may again be reduced to the two stream case. In terms of the quantities from the cases U1-U6,

$$\bar{a}_1 = a_{ion}$$

$$\bar{a}_2 = a_e$$

$$\bar{k}_{D1} = k_{D\sigma} \text{ where } \sigma \text{ refers only to that ion stream which is at rest.}$$

$$\bar{k}_{D2} = k_{De}$$

Figure 5 shows the marginal instability in terms of \bar{k}_{D1}/k_{De} vs U_e/a_e for the U1-U6 cases for which U_e/a_e lies in the same range as in case U (fig.4). Since the ion streams were not ignored when U_e was calculated and both these graphs (fig. 4 and 5) show approximately the same curves for marginal instability it would appear justified to ignore the ion streams with the same streaming velocity as the electron stream.

Figure 6 shows two curves for the marginal instability in terms of $\bar{k}_{D1}/\bar{k}_{D2}$ vs U_e/a_e . The ratio a_{ion}/a_e for the cases U, U1-U6 was 1/172. The lower curve summarizes the U1-U6 cases for which U_e/a_e lie between 1.0 and 4.0. The upper curve is shown for comparison. It shows the marginal instability for the two stream case with different Debye numbers and streaming velocities, but equal thermal velocities. Table 3.3.16 show the values used to plot the figure. U_j refers to the minimum streaming velocity required for instability of the stream with the largest Debye number. Stability is to the left and under the curve for each case.

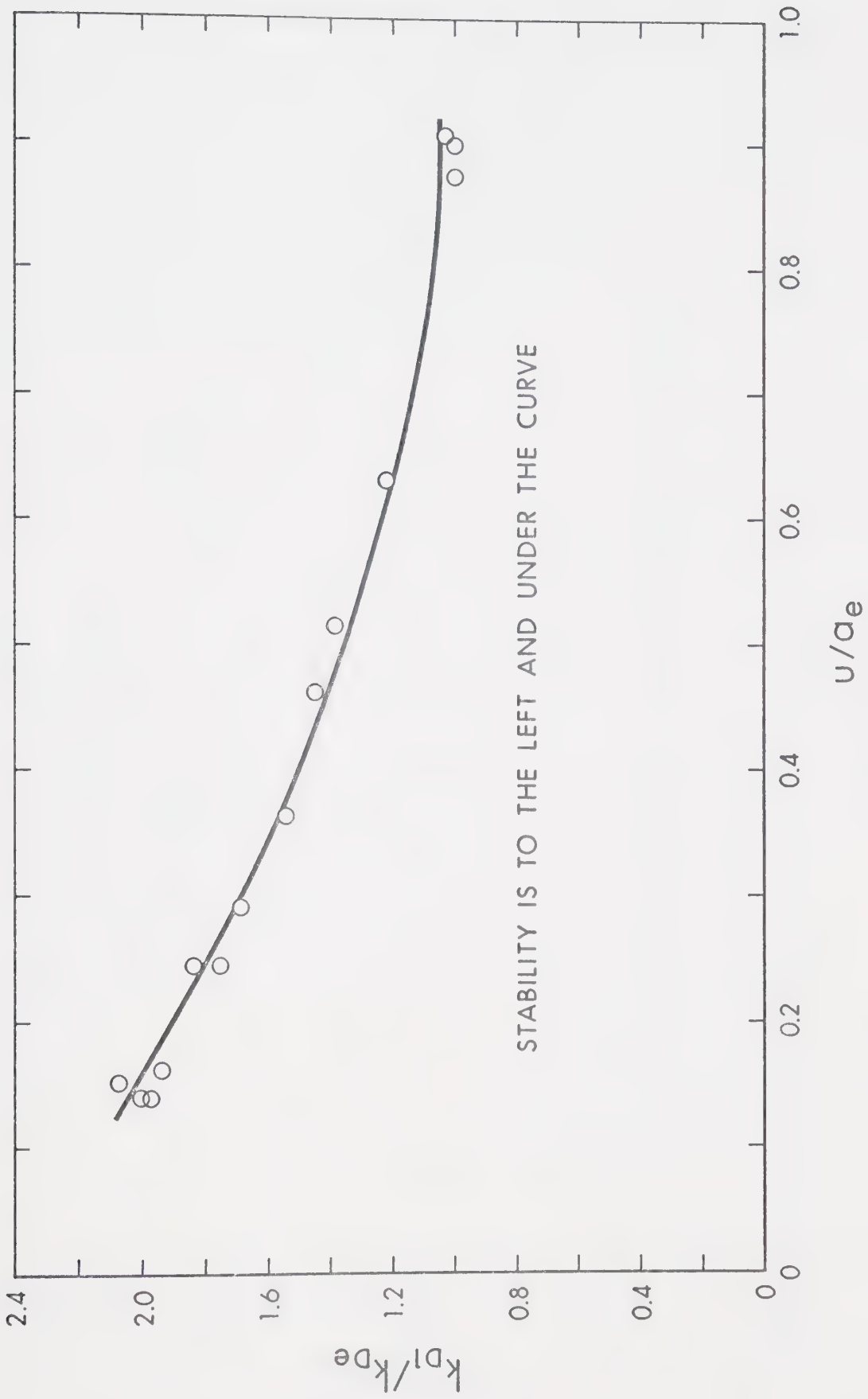


Figure 5 Marginal Stability

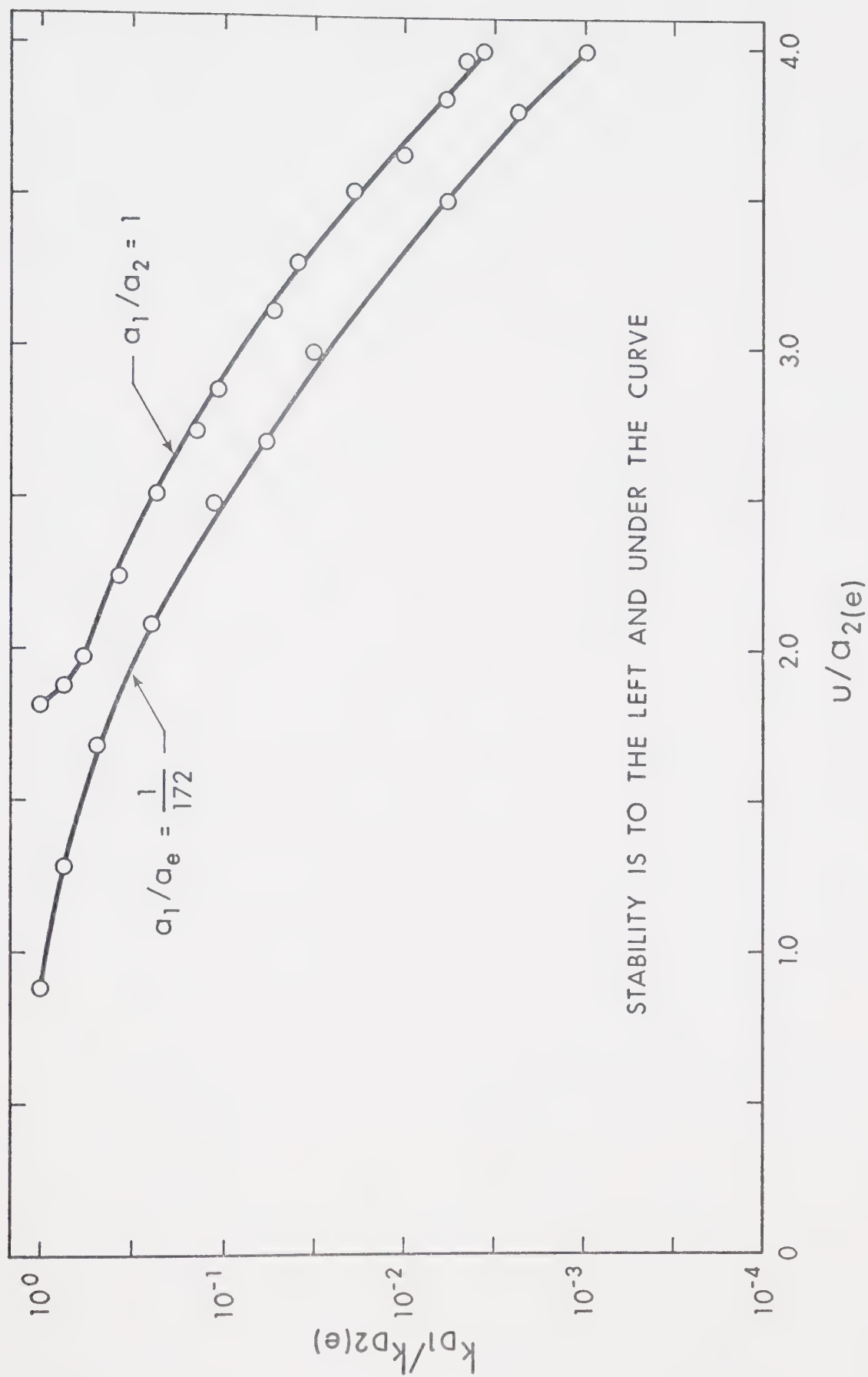


Figure 6 Marginal Stability

TABLE 3.3.16 Instability of a Two-Component Plasma

k_{Di}/k_{Dj}	1.00	0.755	0.586	0.370	0.234	0.145
U_j/a_j	1.84	1.89	1.99	2.27	2.53	2.74
U_i	0	0	0	0	0	0
k_{Di}/k_{Dj}	0.107	0.54	0.039	0.019	0.010	6.5×10^{-3}
U_j/a_j	2.87	3.13	3.30	3.53	3.67	3.84
U_i	0	0	0	0	0	0
k_{Di}/k_{Dj}	4.5×10^{-3}	3.7×10^{-3}				
U_j/a_j	3.98	4.00				
U_i	0	0				

3.4 Multi-component plasmas

This section will explore the problem of a multi-component plasma with one stream having a high thermal velocity, using computer calculations.

As was shown in Section 2.7, a pole z_i of stream i is stabilizing when its thermal velocity is high enough. Further from Section 2.7, this effect is increased when the Debye number k_{Di} is large. In some plasmas, therefore, an increase in thermal velocity causes an otherwise unstable plasma to become stable.

As the first example consider an unstable plasma with the following parameters:

TABLE 3.4.1 Four-Stream Plasmas

Stream:	1	2	3	4
k_{Di}/k_{D2}	0.17	1.0	0.44	0.63
a_i/a_1	1.0	1.0	172	1.0
U_i/a_i	0	2.25	0.004	0

A marginal instability is found at $V_{ph}/a_1 = 0.843$, with poles and their contribution to k^2 as follows.

TABLE 3.4.2 Four-Stream Plasmas

i	z_i	$\text{Im}(k^2)_i$	$\text{Re}(k^2)_i$
1,4	0.843	-0.65	-0.143
2	-1.41	0.65	+0.530
3	-0.0185	0.0	-0.387

Although the pole with the high thermal velocity (z_3) gives a negative contribution to $\text{Re}(k^2)$, the Debye number k_{D3} is not large enough relative to k_{D2} to stabilize the plasma. The contribution of pole z_3 to $\text{Im}(k^2)$ is almost zero. The functions of poles z_1 and z_4 is to cancel the rather large contribution z_2 gives to $\text{Im}(k^2)$. The function of pole z_2 is to cancel the negative contribution z_3 and z_4 gives to $\text{Re}(k^2)$.

The second example shows a case where a plasma is stable.

TABLE 3.4.3 Four-Stream Plasmas

i	1	2	3	4
k_{Di}/k_{D2}	0.141	1.0	0.251	0.519
a_i/a_2	1.00	1.00	1.00	172.
$U_i/a_i(\text{max})$	0.0	4.0	0.0	0.023

As was discussed in Section 2.7, only for phase velocities $\left| \frac{v_{ph}}{a_1} \right| < 4.0$ can there be any instability. For this range, the

pole with the high thermal velocity, z_4 , has a value of approximately -0.02 and so the contribution of this pole to $\text{Im}(k^2)$ is almost zero, and to $\text{Re}(k^2)$ is approximately -0.54. The maximum contribution at any $|V_{ph}/a_i| < 4.0$ to $\text{Re}(k^2)$ of all the poles is denoted by $\text{Re}(k^2)_i$ and is shown below with the appropriate V_{ph}/a_i .

TABLE 3.4.4 Four-Stream Plasmas

i	z_i	$\text{Re}(k^2)_i$	V_{ph}/a_i
1	1.48	+0.011	1.48
2	-1.48	+0.55	2.52
3	1.48	+0.0284	1.48
4	-0.02	-0.54	0.0-4.0

There is a small range, around $V_{ph}/a_i \approx 2.5$ when $\text{Re}(k^2) \geq 0$. The contribution of the poles to $\text{Im}(k^2)$ is denoted by $\text{Im}(k^2)_i$ and shown below with $V_{ph}/a_i = 2.5$.

TABLE 3.4.5 Four-Stream Plasmas

i	z_i	$\text{Im}(k^2)_i$
1	2.52	-0.00
2	-1.48	0.55
3	2.52	-0.00
4	-0.02	0.0

Since $\text{Im}(k^2) \neq 0.0$ when $\text{Re}(k^2) \geq 0$, the plasma is stable. The computer calculations confirmed there was no V_{ph} for which this plasma is unstable.

In the last two examples, the stream with the highest thermal velocity had a small streaming velocity relative to its own thermal velocity $\frac{U_i}{a_i} \approx 0$. The next example shows an unstable plasma where this stream has a larger relative streaming velocity.

TABLE 3.4.6 Three-Stream Plasmas

Streams:	1	2	3
k_{Di}/k_{D2}	0.998	1.0	0.914
a_i/a_1	1.0	1.0	172
U_i/a_i	0.410	0	0.505

A marginal instability is found at $V_{ph}/a_1 = 1.71$. The poles and their contribution to $\text{Re}(k^2)$ and $\text{Im}(k^2)$ are given in the following table.

TABLE 3.4.7 Three-Stream Plasmas

i	z_i	$\text{Im}(k^2)_i$	$\text{Re}(k^2)_i$
1	1.30	-0.85	0.547
2	1.71	-0.30	0.52
3	-0.50	1.15	-0.875

Two streams are needed to balance the contribution to $\text{Im}(k^2)$ made by the stream with the high thermal velocity. This is in contrast to the previous examples where this contribution is almost zero.

Another difference with the previous examples is the effect on the stability of the plasma if the stream with the high thermal velocity is removed. In the previous examples, this removal results in an unstable plasma with a different V_{ph}/a_1 for marginal instability. However, in the last example, the removal results in a stable plasma.

The next example shows a plasma where the value of the highest a_i/a_1 is less than 3.0 compared to 172 in the previous examples.

TABLE 3.4.8 Three-Stream Plasmas

Streams:	1	2	3
k_{Di}/k_{D2}	0.741	1.0	0.944
a_i/a_1	1.0	1.0	2.06
u_i/a_i	0.0	3.31	0.0

A marginal instability is found at $V_{ph}/a_1 = 2.17$. The poles and their contributions to $\text{Re}(k^2)$ and $\text{Im}(k^2)$ are given in the following table.

TABLE 3.4.9 Three-Stream Plasmas

i	z_i	$\text{Im}(k^2)_i$	$\text{Re}(k^2)_i$
1	2.17	-0.03	0.175
2	-1.14	1.04	0.32
3	1.05	-1.01	0.15

It is worthwhile to compare Table 3.4.8 with Table 3.4.1. The values for the streams with $a_i/a_1 = 1.0$ are similar while the

value of a_3/a_1 in Table 3.4.1 is much higher than in Table 3.4.8. The effect of this difference is found by comparing Table 3.4.2 with Table 3.4.9. It is seen that the pole z_3 at marginal instability is almost zero in Table 3.4.2 and large in Table 3.4.9. The result is that this latter pole does not make a negative contribution to $\text{Re}(k^2)$. An instability is found even though the Debye number is large. With the next example, the value of a_3/a_1 is a little higher than in Table 3.4.8.

TABLE 3.4.10 Three-Stream Plasmas

Streams	1	2	3
k_{Di}/k_{D2}	0.741	1.0	0.944
a_i/a_1	1.0	1.0	2.92
u_i/a_i	0.0	3.31	0.0

A marginal instability is found at $V_{ph}/a_1 = 2.41$. The poles and their contributions to $\text{Re}(k^2)$ and $\text{Im}(k^2)$ are given in Table 3.4.11.

TABLE 3.4.11 Three-Stream Plasmas

i	z_i	$\text{Im}(k^2)_i$	$\text{Re}(k^2)_i$
1	2.41	-0.02	0.14
2	-0.90	1.42	0.11
3	0.825	-1.40	-0.25

Every value in Table 3.4.10 is the same as in Table 3.4.8 except the ratio a_3/a_1 . As can be seen in Table 3.4.11, the contribution of

z_3 to $\text{Re}(k^2)$ is negative. The poles z_1 and z_2 contribute positively to $\text{Re}(k^2)$, cancelling the stabilizing contribution of pole z_3 .

The next and last example shows a stable plasma. All parameters are again the same as in Table 3.4.8 except the value a_3/a_1 .

TABLE 3.4.12 Three-Stream Plasmas

Streams	1	2	3
k_{D1}/k_{D2}	0.741	1.0	0.944
a_i/a_1	1.0	1.0	2.98
u_i/a_i	0.0	3.31	0.0

The computer calculations showed the plasma to be stable. To illustrate this, the following two approximations are made to obtain a rough estimate of z_1 when $\text{Im}(k^2)$ is zero.

1. $k_{D3} = k_{D2}$
2. The contribution of pole z_1 to $\text{Im}(k^2)$ is negligible.

By using equation (2.4.5), the above approximations, and the values of the parameters from Table 3.4.12, the following expressions are obtained.

$$z_1 = \frac{\omega}{a_1 k} \quad (3.4.1)$$

$$z_2 = z_1 - 3.31 \quad (3.4.2)$$

$$z_3 = \frac{z_1}{2.98} \quad (3.4.3)$$

Since $\text{Im } Z'(z)$ is even, $z_2 = -z_3$ for a marginal instability to exist. Hence $z_1 = 2.48$. The poles and their contributions to

$\text{Im}(k^2)$ and $\text{Re}(k^2)$ are shown in Table 3.4.13 when $z_1 = 2.48$. The values of k_{Di} that are used in the calculations are the same as in Table 3.4.12.

TABLE 3.4.13 Three-Stream Plasmas

i	z_i	$\text{Im}(k^2)_i$	$\text{Re}(k^2)_i$
1	2.48	-0.02	+0.19
2	-0.83	+1.49	-0.30
3	0.83	-1.33	-0.27

$\text{Re}(k^2)$ is no longer positive, hence no instability exists and the plasma is stable.

The last three examples will now be compared. Tables 3.4.8, 3.4.10 and 3.4.12 are identical except for the value of a_3/a_1 . The following table gives a_3/a_1 together with pole z_1 and $\text{Re}(k^2)$ calculated when $\text{Im}(k^2)$ is zero.

TABLE 3.4.14 Comparisons

	z_1	a_3/a_1	$\text{Re}(k^2)$
Ex.1	2.17	2.06	+0.64
Ex.2	2.41	2.92	0.0
Ex.3	2.48	2.98	-0.38

From Table 3.4.14 it is seen that, for these examples $\text{Re}(k^2)$ is decreased when a_3/a_1 is increased. This confirms that plasmas can be stabilized when the value of a_i is increased. Section 2.7 showed that z_i gives a negative contribution to $\text{Re}(k^2)$ when $a_i > \frac{u_m}{0.924}$. When

divided by a_1 this expression becomes:

$$\frac{a_i}{a_1} > \frac{u_m}{0.924 a_1} \quad (3.4.4)$$

Using the parameters of the previous three examples, with $i=3$, and $\frac{u_m}{a_1} = 3.31$, the expression becomes $a_3/a_1 > 3.58$ when z_3 gives a negative contribution to (k^2) . Tables 3.4.9, 3.4.11 and 3.4.13 show that, in these cases, z_3 is stabilizing for values of a_3/a_1 less than that indicated by equation (3.4.4). The value lies somewhere between 2.06 and 2.92 for these examples. To actually stabilize this plasma, the value a_3/a_1 had to be increased to 2.98 which is still less than the value in equation (3.4.4) for these examples.

This concludes the study of particular examples for the multi-stream case.

Chapter 4

SUMMARY

Instabilities in the infinite, collisionless, homogeneous plasma with no external fields and with an arbitrary number of streams, each stream with its own mass, temperature and streaming velocity has been discussed in this thesis. The physical interpretation of Landau damping and inverse Landau damping has been investigated and it was found that the regimes for which these phenomena were valid were not always the classical ones. It was found that, for one component plasmas, the region of validity of Landau damping includes those disturbances with phase velocity greater than two and one half times the thermal velocity. The regime of marginal inverse Landau damping was found not to include the two stream case.

Bunching, when applied to hot plasmas as well as cold, was shown not to contradict the plasma dispersion relation. (equation 2.6.2). Rather, the parameters involved, debye length, thermal and streaming velocity, were found to support bunching in hot plasmas.

By using the dispersion relation an extensive description was given how temperature, debye length, streaming and thermal velocity changes affect the stability. It was shown that changing any one of these parameters does not necessarily mean increasing or decreasing the stability always the same way. Rather the value of the other parameters of other streams have a direct bearing on the whole plasma stability.

Some graphs have been included to aid in determining the stability of a warm two stream plasma, showing the relationships between various parameters. A method to solve the dispersion relation was reviewed in section 2.6. This method was used to program the computer to solve some cases.

Examples were found where a multi-stream plasma can be made equivalent to a two stream plasma. Various examples were discussed of multi-component plasmas, with one stream always having a higher thermal velocity. Results were compared and found to be in agreement with theoretical limits developed in section 2.7.

The appendix summarizes a method to program the plasma dispersion relation in an economical way, combining several known mathematical formulations of the dispersion relation.

FOOTNOTES

1. Landau, L., Physik Zeits. Sowjetunion 10, 154 (1936).
2. Stix, T.H., "The Theory of Plasma Waves", McGraw-Hill Book Company, New York, (1962).
3. James, C.R. and Vermeulen, F. "A Microparticle Plasma", Canadian Journal of Physics, 46, 855(1968).
4. Schmidt, G. "Physics of High Temperature Plasmas", Academic Press, New York, (1966).
5. Bernstein, I.B. "Plasma Oscillations:II Kinetic Theory of Waves in Plasmas". Nuclear Fusion, 4, 61(1964).
6. Tanenbaum, "Plasma Physics", McGraw-Hill, New York, (1967).
7. Fried, B.D., Conte, S.D., "The Plasma Dispersion Function", Academic Press, New York, (1961).
8. Buneman, O. "Dissipation of Currents in Ionized Media", Physical Review 155, 506(1959).
9. Fried, B.D. and Gould, R.W., "Longitudinal Ion Oscillations in a Hot Plasma", The Physics of Fluids, 4, 139(1961).
10. Gautam, M.S. and Anandaram, M.N., "Computation of the Composition of a Highly Ionized Plasma in Thermodynamic Equilibrium", Canadian Journal of Physics, 49, 492(1971).
11. Franklin, R.N., Research Notes, Plasma Physics, 10, 806(1968).

BIBLIOGRAPHY

- Bernstein, I.B. "Plasma Oscillations: II Kinetic Theory of Waves in Plasmas". Nuclear Fusion, 4, 61(1964).
- Buneman, O. "Dissipation of Currents in Ionized Media", Physical Review 115, 506(1959).
- Franklin, R.N., Research Notes, Plasma Physics 10, 806(1968).
- Fried, B.D. and Goud, R.W., "Longitudinal Ion Oscillations in a Hot Plasma", The Physics of Fluids, 4, 139(1961).
- Fried, B.D., Conte, S.D., "The Plasma Dispersion Function", Academic Press, New York, (1961).
- Gautem, M.S. and Ananandrum, M.N., "Computation of the Composition of a Highly Ionized Plasma in Thermodynamic Equilibrium", Canadian Journal of Physics, 49, 492(1971).
- James, C.R. and Vermeulen, F. "A Microparticle Plasma", Canadian Journal of Physics, 46, 855(1968).
- Landau, L., Physik Zeits. Sowjetunion 10, 154(1936).
- Schmidt, G. "Physics of High Temperature Plasma", Academic Press, New York, (1966).
- Stix, T.H., "The Theory of Plasma Waves", McGraw-Hill Book Company, New York, (1962).
- Tanenbaum, "Plasma Physics", McGraw-Hill, New York, (1967).

APPENDIX

A. Plasma Dispersion Relation

Various expansions exist for the plasma dispersion relation (equation (2.4.15)) and its derivative^{7,11}. Ideally suited for machine calculations are those expansions which make use of continued fractions. A continued fraction is of the form:

$$F = \frac{A_1}{B_1 + \frac{A_2}{B_2 + \dots}} \quad (A.1)$$

Due to convergence problems that are encountered, different expansions are required for different regions of the complex plane.

$$\text{Let } z = x + iy \quad (A.2)$$

Then for $|x| > 5$; and $|y| > 1$,

$$Z(z) = F + \sigma i \pi^{\frac{1}{2}} e^{-z^2} \quad (A.3)$$

Where $\sigma=2$ for $y<0$

$$\sigma = 1 \text{ for } y = 0 \quad (A.4)$$

$$\sigma = 0 \text{ for } y > 0$$

and F is as given by equation (A.1) where

$$A_1 = z$$

$$A_n = -\frac{(n-1)(2n-3)}{2} \quad n=2,3,\dots \quad (\text{A.5})$$

$$B_n = 2n-3/2-z^2 \quad n=1,2,3,\dots \quad (\text{A.6})$$

$$Z'(z) = -2(1 + z Z) \quad (2.6.1)$$

For $|x| + 3|y| < 6$,

$$Z'(z) = F - 2i \pi^{1/2} z e^{-z^2} \quad (\text{A.7})$$

Where F is given by equation A.1 and where

$$\begin{aligned} A_1 &= -2 \\ A_2 &= z^2 \end{aligned} \quad (\text{A.8})$$

$$A_n = \frac{(1-n)z^2}{2} \quad n=3,5,7,\dots$$

$$A_n = \frac{(n-3)}{2} z^2 \quad n=4,6,8,\dots$$

$$\begin{aligned} B_1 &= 1 \\ B_n &= \frac{2n-3}{2} \end{aligned} \quad (\text{A.9})$$

and
$$Z(z) = -\frac{(Z'(z) + 2)}{2z}$$

For $|x| + 3|y| \geq 6$, $|y| > 10^{-4}$

$$Z'(z) = F - 2iz \pi^{1/2} \sigma e^{-z^2} \quad (\text{A.10})$$

where σ is given by equation A.4 and F by equation A.1 where

$$\begin{aligned} A_1 &= -1 \\ A_n &= (1-n)(n-5) \quad n=2,3,\dots \end{aligned} \quad (\text{A.11})$$

$$B_n = 2n - \frac{1}{2} - z^2 \quad n=1,2,\dots \quad (\text{A.12})$$

For $|x| > 6$, $|y| < 10^{-4}$

$$Z'(z) = Z'(x) + iy Z''(x) \quad (\text{A.13})$$

where

$$Z'(x) = -2i \pi^{1/2} x e^{-x^2} - \frac{1}{3/2 - x^2 + F} \quad (\text{A.14})$$

and

$$Z''(x) = -2i \pi^{1/2} (1 - 2x^2) e^{-x^2} + \frac{2 + 2F}{x(3/2 - x^2 + F)} \quad (\text{A.15})$$

Where F in equations A.14 and A.15 are given by equation A.1 where

$$A_n = -n(n + \frac{1}{2}) \quad n = 1, 2, 3, \dots \quad (\text{A.16})$$

$$B_n = 2n + 3/2 - x^2 \quad n = 1, 2, 3, \dots \quad (\text{A.17})$$

The number of terms needed for convergence in equation A.1 varies greatly from about 3 in equation (A.13) to approximately 36 in equation (A.7). Since there is some overlap in the four regions mentioned above, a choice sometimes exists. The places where overlap exists, expansions were used which needed fewer terms for convergence. Expansion A.13 requires the least number of terms, followed by A.10, A.2, and finally A.7. This priority was used to program the plasma dispersion function. Values obtained using this program were in agreement with values tabulated by Fried and Conte⁷.

B30170